The Phase Space Dynamics of Neuronal Systems: I

Model and Experiments.

Arunava Banerjee
Department of Computer Science
Rutgers University
New Brunswick, NJ 08903
arunava@cs.rutgers.edu

November 10, 1997

Abstract

We investigate the phase space dynamics of *local systems* of biological neurons in order to deduce the salient *computational* characteristics of such systems. In this first report, we develop an abstract physical system that models local systems of spiking biological neurons. The system is based on a limited set of realistic assumptions and in consequence accommodates a wide range of neuronal models. Simulations of the model demonstrate that the dynamical behavior of the system is akin to that observed in neurophysiological experiments. In an upcoming report, we shall demonstrate that the dynamics of the model exhibits the classic characteristics of a chaotic system, namely, contraction, expansion, and folding. We view this research as a first step towards understanding the basis for symbolic computation in the brain.

1 Introduction

The construction of an abstract model for a physical system is often a tedious process that can involve numerous cycles of generation and testing of hypotheses till a satisfactory compromise between simplicity and predictive accuracy is achieved. The process is rendered all the more problematic by the fact that in any first attempt at understanding the nature of a complex physical system little is known in advance about which features of the given mechanism are crucial with regards to the phenomenon under investigation, and therefore demand modeling, and which features can safely be regarded as superfluous.

The study of the *brain as a computational device* is a classic example of a problem that abounds in such difficulties. At the highest level of abstraction the brain can be viewed as a system that is composed of numerous copies ($\approx 10^{11}$ in the human brain) of a lone functional unit, the neuron. This outlook however, changes drastically when the brain is viewed at a more concrete level. Physiological and anatomical investigations have established that neurons in the brain come in an overwhelming variety of shapes, forms, and functional

types. Furthermore, there is extensive evidence both of structure and the lack thereof in the layout of connections between individual neurons.

Before one can construct an abstract model, one has to pick parameters to delineate the scope of the model. Whereas some of the choices will be motivated by the objectives of the investigation, others will have to be made arbitrarily. In the context of the brain these considerations include (1) the structural level at which the brain shall be modeled, (2) the accuracy with which the physiological neuron shall be modeled, and (3) the accuracy with which various anatomical types of neurons shall be modeled. We discuss our position on each of these issues at length in the coming sections. First however, we review the conflicts between the major viewpoints in the field, and in the process situate our own research agenda.

Connectionism vs. The Classical Approach

A feud has been raging between the connectionist school and the classical school of cognitive architecture ever since the inception of the connectionist school in the late fifties (Rosenblatt 1958; Minsky and Papert 1972) and its remergence in the mid eighties[1] (Rumelhart and McClelland 1986). There has also been a widening gap between the class of problems addressed by the respective schools of thought. The classical school with its foundations in the symbol system hypothesis, (Newell and Simon 1976; Newell 1980) has steadfastly rejected the tenets of the connectionist school, arguing that the latter is not committed to a symbolic level of representation or to a language of thought (Fodor and Pylyshyn 1988).

In our opinion the controversy, at least in its present form, stems from the state of infancy of the field of connectionism. Both classicists and connectionists are *representationalists*, i.e., both believe that there are states of the mind that encode states of the world. While the classical school concerns itself with the exact manner in which these mental states ("symbols") are manipulated (presupposing of course that such can be modeled after the Turing and Von Neumann machines), it falls on the connectionists to first determine where these symbols exist in the physical processes of the brain before they can begin investigating their dynamics.

Neuroscience vs. Connectionism vs. The Classical Approach

Studies in connectionism have so far been confined to relatively simple notions of the *neuron* and of *networks*. The dynamics of such networks show little similarity to the dynamics that neuroscientists routinely observe in the brain. Consequently, neuroscience has rejected connectionism as being too simplistic. In an effort to find common ground with the classical approach, some connectionists have attached, albeit in an ad hoc manner, symbolic interpretations to the states of their networks. The elementary manner in which these networks manipulate symbols have led the classicists to reject connectionism on similar charges.[2]

The fact remains, however, that a brain theory without a bridge between the physical level and the symbolic level is inherently incomplete. Furthermore, neither neuroscience has

[1] Initiated by a breakthrough in learning on multi-layer perceptrons through error back-propagation.

[2] It is not claimed that these networks are computationally weaker than the FSM or the TM; only that they have been put to very elementary use in systems constructed by connectionists.

a tenable theory for the location of symbols in the processes of the brain[3], nor does the classical school for a symbol level description of the mind.

Computer Simulation in Neuroscience

The search for coherent structures in the dynamics of neuronal systems has seen a surge of activity in recent times (Krüger 1990a; Basar 1990; Aertsen and Braitenberg 1992). Armed with faster and more powerful computers, scientists are replicating salient patterns of activity observed in neuronal systems in phenomena as diverse as motor behavior in animals, and oscillatory activity in the cortex. The models of the neurons as well as those of the networks are considerably more realistic in these cases. There is an emphasis on simulation and it is hoped that analytic insight will be forthcoming from such experimentation.

Our Approach

While entertaining similar objectives, our research differs considerably in its approach. The goal of our research is to eventually answer two very crucial questions.

1. Are there *coherent* structures in the dynamics of neuronal systems that can denote *symbols*, and

2. If such structures exist, what restrictions do the dynamics of the system at the physical level impose on the dynamics of the system at the corresponding abstracted symbolic level.

Whereas these objectives conform with the bottom-up philosophy, we believe that answers to these questions can be obtained primarily through an extensive *analysis* of the phase space dynamics of an abstract system whose dynamical behavior matches, sufficiently, that of the biological system (the brain or any part thereof).

This emphasis on *analysis* of the phase space dynamics of an abstract system imposes various constraints on the mathematical formulation of the system. In order for the system to be amenable to analysis, it is vital that the system evaluate favorably with respect to the following criteria.

- Tractability: The manner in which an abstract system is formulated has, in general, a sizable impact on how discernible the salient behavioral characteristics of the system are. A good abstract model will readily reveal any salient behavioral traits that the actual physical system might possess.

- Behavioral Proximity The dynamical behavior of the model must resemble that of the actual physical system being modeled. It is after all the physical system that one wishes to make claims about. It makes little sense to study an abstract system that is not representative of the physical system being investigated.

[3]Hebbian Cell Assemblies (Hebb 1949) and Synfire Chains (Abeles 1982) are various attempts at resolving this problem.

- Generality: The brain viewed at a concrete level is quite inhomogeneous. This fact is exemplified in the contrast between the orderly connection patterns in the cerebellar cortex and the unstructured tangle of connections in the cerebral cortex. In order to discern the similarities and differences between the dynamics of these systems, one must be able to exercise the same abstract system to model either physical system. Generality becomes all the more necessary in light of the fact that inhomogeneity in the brain can be traced all the way back to the cellular level. Uniform modeling of anatomically distinct neurons necessitates generality in the abstract system.

The above criteria are not entirely orthogonal to one another. Whereas transparency calls for simplicity in the model, behavioral proximity entreats the opposite. The abstract model presented in this paper is the outcome of several attempts on our part to strike a balance between these criteria.

The paper is structured as follows. In section 2, some of the models of neurons that have been proposed are reviewed, following which our model is presented in detail. In Section 3 the phase space for a neuronal system is constructed based on restrictions imposed by our model of the neuron. The section concludes with a detailed description of the velocity vector field that overlays the phase space. Section 4 presents results from simulations of the system. The purpose of these simulations is two-fold. First, we aim to demonstrate that the dynamics of the abstract system is, in general, consistent with that observed in the real system, and second, we aim to highlight salient behavioral characteristics of the system that we then plan to explore analytically. This being the first of a series of technical reports, the paper lacks a conclusion and future research sections.

2 Models Of The Neuron

The simplest model of the neuron that has received widespread attention in the connectionist literature is the *threshold unit*. The response of a threshold unit to input $\langle x_1(t), x_2(t), ...x_n(t)\rangle \in \{0,1\}^n$ is given by

$$y(t+1) = H(\sum_{i=1}^{n} w_i.x_i(t) - \theta)$$

where H(.) is the unit step function, w_i are weights assigned to the input lines and θ is the threshold of the unit. In their pioneering work McCulloch and Pitts (1943) demonstrated that a network consisting of such units with a synchronous update policy could implement logic gates and therefore simulate a finite automaton. Threshold networks have since then been analyzed in great detail by Complexity theorists.

In a slight extension to this model, the unit step function is replaced by a smooth sigmoid and the inputs are allowed to take real values between 0 and 1. Networks comprising of such units have been growing in popularity ever since it was shown that such networks can be *trained* to associate a set of inputs with an arbitrary set of outputs (Rumelhart, Hinton and Williams 1986).

While networks consisting of such units have generated great interest, the units themselves do little justice to biological neurons. A typical biological neuron transforms a spatio-temporal sequence of spikes impinging on its numerous synapses into a temporal sequence

of spikes on its axon. Incoming spikes diffuse into the cell body in the form of graded potentials with temporal decays and are integrated by the neuron at its axon hillock. The spike response of the cell to the potential at its hillock reveals both a thresholding and a refractory phenomenon at play.

Models of the neuron that operate in a fashion similar to that described above are often called integrate-and-fire models. Although belonging to the same class, the various integrate-and-fire models differ sharply in complexity. The simplest model (variously called the Lapique Model, the leaky integrator, and the forgetful integrate and fire model) disregards the spatial aspect of the nerve cell entirely by lumping together the soma and dendrites in one representative circuit. The subthreshold behavior of the model is given by

$$C\frac{dV}{dt} + \frac{V}{R} = I(t)$$

where V represents the cross-membrane potential, C the capacitance and I the injected current. The model is completed by imposing the condition that an action potential be generated by the cell when $V(t)$ reaches the threshold $\theta(t)$. Refractoriness is implemented by defining $\theta(t)$ as

$$\theta(t) = \begin{cases} \infty, & t_i < t < t_i + t_R, \\ \theta, & otherwise. \end{cases}$$

where t_R represents the *absolute refractory period.* The response of the Lapique model to various input configurations has been explored extensively. We refer the interested reader to (Tuckwell 1988) for a survey of these results.

A more realistic model that takes into account the spatial aspects of the dendrites has been developed in (Rall 1960). Here, cable theory is applied to model passive conductance in the dendritic abortization. Active ion transports that result in spike generation are however, not modeled. The response of Rall's model to various input configurations has also been studied extensively and we refer the interested reader to (Tuckwell 1988). In this section we discuss the model's response to one set of boundary conditions for later use in our simulations.

The cable equations are a simple pair of p.d.e's

$$-\partial i = (g_m v_m + c_m \frac{\partial v_m}{\partial t})\partial x$$

$$\frac{\partial v_m}{\partial x} = -(r_i + r_o)i = -ri$$

where v_m is the cross-membrane potential, g_m the membrane conductance per unit length, c_m the membrane capacitance per unit length, r the compound resistance per unit length and i the current flow through the cable. This set of p.d.e's can be solved in various ways. One such solution (MacGregor and Lewis 1977) uses the Laplace transform method to give

$$v_m(x,s) = v(0,s)\cosh[\sqrt{rg_m + rc_m s}\ x] - [\sqrt{\frac{r}{g_m + c_m s}}]i(0,s)\sinh[\sqrt{rg_m + rc_m s}\ x]$$

$$i(x,s) = i(0,s)\cosh[\sqrt{rg_m + rc_m s}\ x] - [\sqrt{\frac{g_m + c_m s}{r}}]v(0,s)\sinh[\sqrt{rg_m + rc_m s}\ x]$$

Assuming a short circuit at the soma, i.e., $v_m(l,s) = 0$, a synaptic impulse at the near end, i.e., $i(0,s) = I_{syn}(s) = Q$, and a semi-infinite dendrite ($l \to \infty$) so that higher order terms in the solution may be disregarded, one arrives at the solutions,

$$i(x,t) = [\frac{Q\sqrt{rc_m x^2}}{2\sqrt{\pi t^3}}]e^{-rc_m x^2/4t}e^{-(g_m/c_m)t}$$

$$v_m(x,t) = [\frac{Qr}{\sqrt{rc_m x^2 \pi t}}]e^{-rc_m x^2/4t}e^{-(g_m/c_m)t}$$

The potential response at the soma to an impulse Q at $t = 0$ (representing the arrival of a spike at the synapse) can therefore be summarized as

$$v(t) = \frac{\alpha Q}{\sqrt{t}}e^{-\beta/t}e^{-\gamma t}$$

where α, β, and γ are constants that depend on the various spatial (distance of synapse from the soma) and electronic (c_m, g_m, r) properties of the dendrite.

In order to determine how reasonable the boundary conditions are that lead to the above solution, we compared it to simulations of *subthreshold* response in a neuron to synaptic inputs on NEURON v2.0 (Hines 1993). The soma and axon of the neuron were modeled as a single segment satisfying the HH equations. Six dendritic branches connected irregularly to form a tree of depth two were also attached to the soma. Synaptic inputs were applied at various locations on the dendrites and the responses at the soma were noted. We found a good fit between these results and the above solution when appropriate values were chosen for α, β, and γ. Figure 1 displays the result of one such experiment.

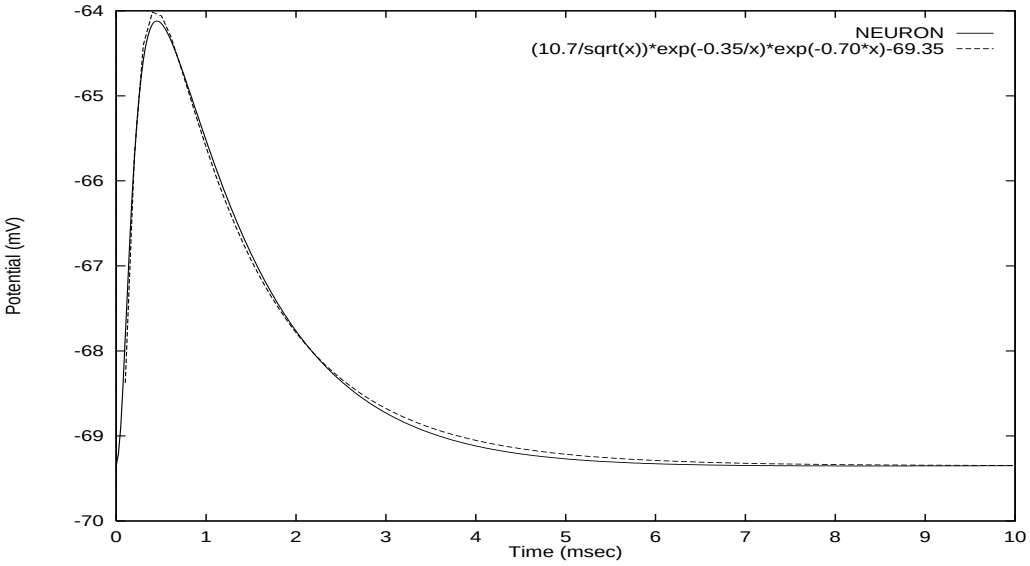

Figure 1: Single PSP: Comparison between simulation on NEURON and the solution.

One of the advantages of using cable theory to model subthreshold response at the soma is that the equations are *linear*. In other words,

if V_1 is the solution of the equation
$V_t = V_{xx} - V + I_1$, with initial value $v_1(x)$ (I_1 is introduced as injected current density at $\langle x, t \rangle$),

and V_2 is the solution of the equation
$V_t = V_{xx} - V + I_2$, with initial value $v_2(x)$ and the same boundary conditions,

then the solution of
$V_t = V_{xx} - V + I_1 + I_2$, with the same boundary conditions and initial value $v_1 + v_2$ is $V(x,t) = V_1(x,t) + V_2(x,t)$.

While spatio-temporal integration of PSP's on a single dendritic branch is linear (the consequence of the linearity of cable theory), spatio-temporal integration of PSP's on an entire dendritic tree is in general not so. It has however, been shown in (Walsh and Tuckwell 1985) that if all dendritic terminals are at the same distance from the origin, and at all branch points on the dendritic tree $diameter^{3/2}_{parent-cylinder} = \sum diameter^{3/2}_{daughter-cylinder}$, then the entire dendritic tree can be mapped onto a single nerve cylinder; in which case integration of PSP's over the entire dendritic tree becomes linear. We tested the results of linear summation of PSP's against simulations on the toy neuron described above (the toy neuron violated these assumptions) and found an agreeable fit, as shown in figure 2.

Rall's model does not account for generation of action potentials, and therefore, in order to complete the model one has to impose a threshold and refractoriness.

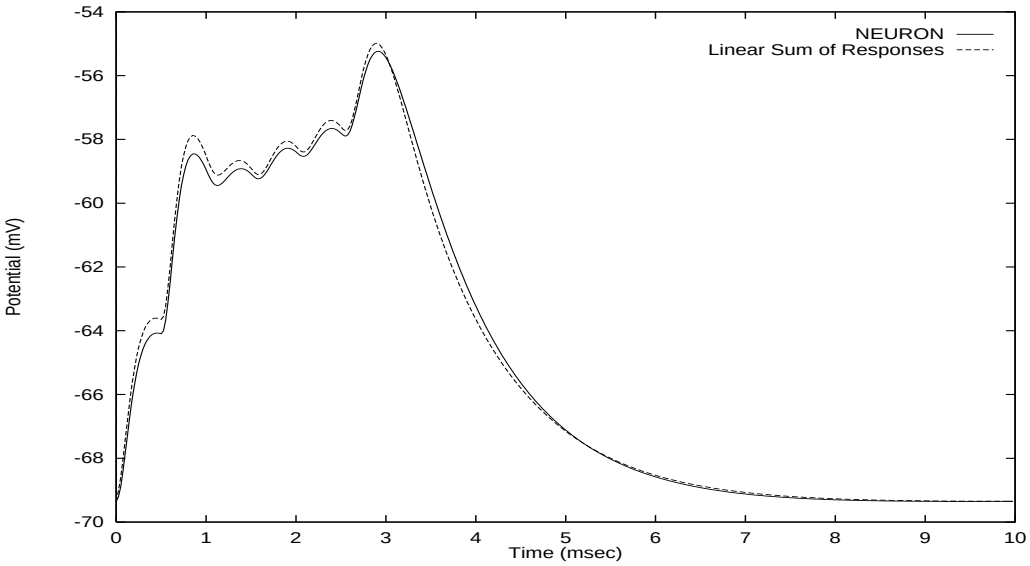

Figure 2: PSP integration: Comparison between simulation on NEURON and linear sum of solutions.

Finally, we touch upon the Hodgkin-Huxley model that accounts for both subthreshold and superthreshold responses in a neuron (Hodgkin and Huxley 1952a-d). Here, non-linear terms are added to the cable equations to model the dependence of sodium and pottasium conductance on the cross-membrane potential. While these equations account for action

potentials, refractoriness, and accommodation in a neuron, their complexity makes it prohibitive to incorporate into a theory of neuronal *systems*. In spite of attempts to reduce the complexity of these equations while maintaining their qualitative properties (Fitzhugh 1961; Nagumo, Arimoto, and Yoshizawa 1962), the prospect of their inclusion into *analytical* models for neuronal systems remains bleak.

Several stochastic (as opposed to deterministic) models have also been proposed for the activity of neurons which are not discussed here. We have chosen a deterministic model for the neuron for reasons that we describe in the following section.

Our Model Of The Neuron

The level of *detail* at which one expects to encounter a phenomenon of interest should, under ideal circumstances[4], dictate the choice between a stochastic and a deterministic model for a physical system. Very often, however, one has little option but to use a stochastic model since complete knowledge about the system is lacking. Under such circumstances, the price is the limited scope of questions that the abstract model can answer. It is clear, however, that whatever the level of one's knowledge about a physical system, an abstract model is virtually useless unless its resolution is higher than that of the phenomenon of interest.

There are numerous good arguments in favor of choosing a stochastic model for describing neuronal activity. First, in most experimental studies of the activity of neurons in their natural environment, i.e. the brain, very little, if anything, is known about the inputs to the cell under study (the enormous number of synapses on a cell makes this an almost impossible task). Second, spike train recordings appear to be entirely random, with distributions matching that of poisson processes. Finally, randomly occuring miniature end plate potentials (m.e.p.p) have been observed in experiments, (Fatt and Katz 1952) suggesting that neurons are noisy.

The case against stochastic modeling however, is stronger. The most serious concern stems from mounting evidence that information about stimulus is contained in the higher resolution ISI's[5] of spike trains and not in the lower resolution spike frequencies (Krüger 1990b; Mainen, and Sejnowski 1995; Bair, and Koch 1996). Since the temporal sequence of ISIs is abstracted away in a stochastic model, there is little hope that such a model will shed light on information processing in neuronal systems. Second, while m.e.p.p do exist their mean amplitude is about 0.5mV as compared to a mean amplitude of 50-70 mV for an average e.p.p elicited by the arrival of a spike at a synapse. Third, (Softky and Koch 1992) have shown that the use of a stochastic model for neuronal activity leads to results that are inconsistent with recorded data. Finally, as shall be demonstrated in section 4, our deterministic model does produce spike trains that are seemingly random.

Before describing our model, we make the following observations about biological neurons.

- The neuron is a finite precision machine in the sense that the depolarization at the soma that elicits an action potential is a finite range ($T \pm \epsilon$) and not a precise value (T).

[4] When absolute knowledge about the system is available.

[5] Inter Spike Intervals

- The effect of a synaptic impulse at the soma has the characteristic form of an abrupt increase or decrease in potential followed by a longer exponential-like *decay* towards the resting level.
- The ISI for any given neuron i is bounded from below by its *absolute refractory period* (r_i), i.e., no two spikes originate closer than r_i in time.

Based on these facts, we construct our model of the neuron as follows.

(i) **Spikes**: Spikes are the sole carriers of information. Spikes are identical except for their spatio-temporal location (Spikes are defined as point objects. Even though action potentials are not instantaneous, one can always assign them occurance times, which may for example be the time at which the cross-membrane potential reached the threshold (T).).

(ii) **Cross-Membrane Potential**: For any given neuron we assume an *implicit*, C^1, *everywhere bounded function* $P^*(\vec{x_1}, \vec{x_2}..., \vec{x_m})$ that yields the *current* cross-membrane potential at the soma. ($1..m$ represent the synapses, and $\vec{x_i} = \langle x_i^1, x_i^2, ..., x_i^k, x_i^{k+1}, ...\rangle$ is a *denumerable* sequence of variables that represent the arrival times of spikes at synapse i since infinite past with present set at t=0).

$P^*: \mathbb{R}^\omega \rightarrow \mathbb{R}$ accounts for the entire spatio-temporal aspect of the neuron's response to spikes. Consistency requires that either the domain of definition for $P^*(.)$ be restricted to $\forall i\ 0 \leq x_i^1 \leq x_i^2 \leq ...$, or $P^*(.)$ be constrained to be symmetric with respect to variables in $\langle x_i^1, x_i^2, ..\rangle\ \forall i$ in the domain $\mathbb{R}^\omega$.

(iii) **Effectiveness of a Spike**: After the effect of a spike at the soma decays below (ϵ/m), where ϵ is the range of error of the threshold and m the number of synapses on the cell, its effectiveness on that neuron expires. This can reasonably be assumed because (a) the total effect of a set of spikes on the soma is almost linear in their individual effects when such effects are small $\approx (\epsilon/m)$, and (b) the neuron is a finite precision machine. This criterion, in essence, bounds from above the period over which a spike impacting at a given synapse is effective on a neuron.

We represent this formally by imposing restrictions on P^*, namely,

- For each synapse i,
  $\exists \tau_i$ such that $\forall t \geq \tau_i$ and $\forall j\ \frac{\partial P^*}{\partial x_i^j}\ |_t = 0$ irrespective of the values assigned to the other variables.
- For each synapse i,
  $\forall j\ \frac{\partial P^*}{\partial x_i^j}\ |_{t=0} = 0$ irrespective of the values assigned to the other variables.
- $P^*(\tau_1, \tau_1...., \tau_2, \tau_2...., \tau_m, \tau_m....) = 0$
- $P^*(0, 0...., 0, 0...., 0, 0....) = 0$

The first criterion enforces that if $\forall$ synapse $i\ \exists n_i$ such that $\forall j > n_i,\ a_i^j \geq \tau_i$ then $P^*(\vec{a_1}, \vec{a_2}, .., \vec{a_m}) = P^*(\vec{a_1}', \vec{a_2}', .., \vec{a_m}')$ where $\vec{a_i}'$ is derived from $\vec{a_i}$ by setting all values after index n_i to τ_i. The second criterion results from $P^*(.)$ being a C^1 function and

$\frac{\partial P^*}{\partial x_i^j} \mid_{t<0} = 0$ which reflects the fact that a spike that has not yet reached a synapse can have no effect on the cross-membrane potential. The third and forth criteria enforce that the resting state (set at 0) is the same before and after the arrival of spikes.

(iv) **Finite dimensionality**: The function characterizing the cross-membrane potential can, as a result, be defined over a finite dimensional space by noting that at any synapse i, spikes arrive at intervals bounded from below by r_i (the absolute refractory period of the neuron pre-synaptic to i) and therefore at most $n_i = \lceil \tau_i / r_i \rceil$ variables can have values less than τ_i. Based on (iii) above we can define,
$P(x_1^1, ...x_1^{n_1}, x_2^1, ...x_2^{n_2}, ...x_m^1 ...x_m^{n_m}) =$
$P^*(x_1^1, ...x_1^{n_1}, \tau_1, \tau_1, ..., x_2^1, ...x_2^{n_2}, \tau_2, \tau_2, ..., ..., x_m^1 ...x_m^{n_m}, \tau_m, \tau_m ...)$
and utilize $P(.)$ instead of $P^*(.)$ to represent the current membrane potential. We call this the *finite memory* criterion. [6]

(v) **Threshold and Refractoriness**: A simple model is assumed for the generation of a spike at a given soma, i.e., a spike is generated when $P(.) = T$ (the cross-membrane potential reaches the threshold). This simple construction, however, rules out modeling *accommodation* in the neuron.

It might appear, at first glance, that by retaining merely a limited duration account of the past record of *incoming* spikes, the model has in effect forsaken the capacity to compute any history of *outgoing* spikes[7], and can therefore not model refractoriness. However, since the phenomenon of refractoriness can also be bounded in time based on considerations identical to (iii) above, the situation can be remedied by extending each τ_i by an appropriate interval of time, namely, the period of effectiveness of the refractory effect of any outgoing spike, and recomputing each n_i.

While this demonstrates that in principle $P(.)$ can account for refractoriness, we do not pursue this course because, as will become clear in the next section, our model will have at its disposal a limited history of outgoing spikes of all neurons. Anticipating this, we partition $P(.)$ into its functionally distinct parts, $P(.) = P_{Afferent}(incoming\ spikes) + P_{Refractory}(outgoing\ spikes)$. This allows for uniform modeling of refractoriness by attributing it to the inhibitory effects of outgoing spikes. Since $P(.)$ is assumed to be C^1, instead of the widely used

$$P_{Refractory}(t) = \begin{cases} (T_\infty - T_0)e^{-(t/\lambda)}, & t > 0, \\ 0, & otherwise. \end{cases}$$

[6] A few technicalities should be mentioned here. The definition of P^* assumes that spikes have been arriving at each synapse since $t = -\infty$. If the number of spikes on any synapse is finite over the time $(-\infty, 0)$, then a denumerable number of dummy variables can be added to extend the function's domain to $\mathbb{R}^\omega$. Moreover, for any dummy variable x, $\frac{\partial P^*}{\partial x}$=0 is consistent with the constraints imposed on P^*. Second, one must be careful to note that the restrictions on P^* imply that a neuron is not sensitive **at present** to spikes that arrived before a specific time, not that the neuron was never sensitive to such a spike for there was surely a time when the arrival time of the spike was less than the given bound.

[7] In question is not whether the model can predict if the neuron will spike at present but whether it can predict if the neuron spiked in the past and if so at what times.

we use a C^1 function that decreases quickly from zero and then decays rapidly back to zero, and expand the criteria for the generation of a spike to $P(.) = T$ and $\frac{dP(.)}{dt} \geq 0$.[8]

The above model of the neuron does not insist on a specific function, only that the particular function possess certain qualitative properties. It is our hope that by retaining this level of generality, we can pose questions that are more basic, such as, to what extent would the dynamics of a neuronal system be affected if the potential function $P_{Afferent}(.)$ were to be replaced by any arbitrary function that is both C^1 and is unimodal[9] with respect to all variables. Besides, making a model more specific by resorting to explicit functions is a much easier task than making it more general.

We must mention here that in spite of the generality of the cross-membrane potential function, this model remains some distance from an accurate depiction of the biological neuron. Accommodation is one of the important traits of a biological neuron that is not modeled. Furthermore, there exist neurons that respond to excitation with bursts of spikes instead of a single action potential. We can only hope that not much is lost in terms of the salient behavior of the system at our leaving out such details.

3 The Phase Space

The analysis in the previous section focussed on the post-synaptic neuron and its cross-membrane potential function. We now repeat this analysis focusing on the pre-synaptic neuron.

Given any neuron j, let $i = 1...k$ denote the set of synapses that the neuron is pre-synaptic to, i.e., the set of synapses that receive spikes from the given neuron. Let λ_i denote the time it takes for a spike generated at the soma of the neuron to reach synapse i. Furthermore, as before, let τ_i denote the time interval over which a spike impinging on synapse i is effective on the corresponding post-synaptic neuron, and r_j denote the absolute refractory period of the given pre-synaptic neuron.

Since its inception, the maximum time period over which a spike is effective on at least one post-synaptic neuron is then given by $\Upsilon_j = max_{i=1}^{k}\{\lambda_i + \tau_i\}$. Consequently, the given neuron can, at any time, have at most $n_j = \lceil \Upsilon_j / r_j \rceil$ effective spikes.

Returning to the cross-membrane potential function for the post-synaptic neuron, we note that this shift in emphasis onto the pre-synaptic neuron induces a few small changes in the definition of $P(.)$. Previously, parameter x_i^j represented the time since the arrival of a spike at synapse i. We now define x_i^j as the time since the inception of the spike at the corresponding pre-synaptic neuron. This is accomplished by a mere translation of the function along all axes so that the previous origin is now located at $(\underbrace{\lambda_1, \lambda_1, ...}_{n_1 \ times}, ..., \underbrace{\lambda_m, \lambda_m, ...}_{n_m \ times})$. The requirement that $\frac{\partial P^*}{\partial x_i^j} \mid_t = 0$ for $0 \leq t \leq \lambda_i$ continues to hold because of the manner in which $P(.)$ was previously defined. The number of variables associated with some synapses do, however,

[8] $\frac{dP(.)}{dt} = \sum_{i,j}^{spikes} \frac{\partial P(.)}{\partial x_i^j}$. $P(.) = T$ is crossed twice, once when the spike is generated and once when the refractory effect of the spike kicks in. The quick decrease in the refractory curve is made sharp enough to ensure that the only significant factor in $\frac{dP(.)}{dt}$ during its downwards journey is $P_{Refractory}(.)$.

[9] Increases monotonically, then decreases monotonically.

increase because all synapses that share the same pre-synaptic neuron j are consistently assigned n_j variables. This is once again achieved trivially by setting appropriately fewer variables to τ_i in $P^*(.)$ in item (iv) of the previous section.

We note immediately from the above description that the state of a *system* of neurons can be specified completely by enumerating the position of the n_j (or fewer) most recent spikes associated with each neuron j that were generated in the past within Υ_j time from the present. On the one hand, such a record specifies the exact location of all spikes that are still situated on the axons of respective neurons, and on the other, combined with the potential functions, it specifies the current state of the soma of all neurons. This description has the added advantage that in explicitly recording the position of all spikes (incoming and outgoing being merely a matter of perspective), $P(.)_{Refractory}$ can be defined directly on the domain, i.e., without first referring to $P(.)_{Afferent}$ to compute the positions of outgoing spikes from the positions of incoming spikes. While it is assumed here that neurons do not receive external inputs, incorporating such is merely a matter of introducing additional neurons whose state descriptions are identical to that of the external input.

This gives us the following initial description of the state of a neuron: the state of neuron j at any given moment in time is given by the n_j-tuple $\langle x_j^1, x_j^2, ...x_j^{n_j}\rangle \in [0, \Upsilon_j]^{n_j}$ where Υ_j, and n_j are as described above. Each component x_j^l ($l = 1..n_j$) in the n_j-tuple represents the time since the inception of the lth spike at the soma of neuron j. Since n_j is merely an upper bound on the number of spikes that were generated within Υ_j time from the present, it is conceivable that fewer than n_j spikes satisfy this criterion, in which case the remaining components are set to Υ_j. In other words, a spike continues to age (the value of the component grows) until it reaches the bound Υ_j at which point it ceases to age.[10] The resultant phase space for the neuron is the *closed* n_j-cube, $[0, \Upsilon_j]^{n_j} \subset \mathbb{R}^{n_j}$.

It is clear, however, that this initial description is neither complete nor uniquely representative of the state of a neuron. First, the *finite length* description of the state of a neuron implies that a variable is reused to represent a new spike when the effectiveness of the old spike it represented terminates. The precondition of *continuity* in phase space dynamics therefore requires that Υ_j be identified with 0.[11] Second, if $\langle x_j^1, x_j^2, ..., x_j^{n_j}\rangle$ and $\langle y_j^1, y_j^2, ..., y_j^{n_j}\rangle$ are two vectors that satisfy the criterion that $\exists\sigma$ such that $\sigma(\vec{x_j}) = \vec{y_j}$ (σ being a permutation) then whereas $\vec{x_j}$ and $\vec{y_j}$ are two distinct points in the space $[0, \Upsilon_j]^{n_j}$, they represent the same state of the neuron (which variable represents a spike is immaterial). This stipulates that all permutations of a vector be identified with the same state.

In what follows we construct a differentiable manifold that satisfies both these criteria. The construction is divided into two stages. At the end of the first stage the first criterion is satisfied and at the end of the second stage the second criterion is satisfied. Informally, the first stage transforms the interval $[0, \Upsilon_j]$ into the unit circle S^1. In other words, at the end of this stage spikes are represented as complex numbers of modulus one. The second stage computes a complex polynomial whose roots match, identically, the above set of complex numbers. By retaining only the coefficients of this polynomial, all order information is eliminated.

[10] This is just a different way of stating criterion (1) of item (iii) or criterion (iv) in the previous section.

[11] A variable with value Υ_j (ineffective spike) is set to 0 when it is assigned to a new spike.

Stage 1

We impose on the manifold $\mathbb{R}$ the equivalence relation: $x \sim y$ if $(x - y) = a.\Upsilon$, where $x, y \in \mathbb{R}$ and $a \in \mathbb{Z}$, and regard $\mathbb{R}/\sim$ with its standard quotient topology. The equivalence class mapping $\pi : \mathbb{R} \to \mathbb{R}/\sim$ can be identified with $\pi(t) = e^{\frac{2\pi it}{\Upsilon}}$ and it is evident that $\mathbb{R}/\sim$ is both Hausdorff, and has a countable basis of open sets (π is *open.*). π essentially identifies the quotient space $\mathbb{R}/\sim$ with $S^1 = \{z \in \mathbb{C} |\ |z| = 1\}$.

We therefore apply the following transformation to the initial description, namely, $\langle x^1, x^2, ..., x^n\rangle \to \langle e^{\frac{2\pi ix^1}{\Upsilon}}, e^{\frac{2\pi ix^2}{\Upsilon}}, ..., e^{\frac{2\pi ix^n}{\Upsilon}}\rangle$. The new phase space is $T^n = \underbrace{S^1 \times S^1 \times ....S^1}_{n\ times}$ the *n-torus*. It is clear that T^n satisfies the first criterion.

Stage 2

The fact that the set G=$\{\sigma |\ \sigma$ is a permutation of n elements$\}$ forms a *Group* motivates the approach that the *orbit space* T^n/G of the *action* of G on T^n be considered. The problem with this approach, however, is that G does not act *freely*[12] on T^n. This is demonstrated in the example: if $x = \langle z_1, z_2, ..., z_n\rangle \in T^n$ is such that $z_1 = z_2 = ... = z_n$ then $\forall g \in G\ gx = x$. The quotient topology of T^n/G therefore does not inherit the locally Euclidean structure of T^n.

Hence, we take a different approach wherein we explicitly construct the space as a subset of the Euclidean space and endow it with the standard topology. Our goal is then to transform the space, $T^n = \{\langle z_1, z_2, ..., z_n\rangle |\ \forall i\ z_i \in \mathbb{C},\ |z_i| = 1\}$ to one wherein information about the order of terms is absent.

The construction is based on the crucial observation that the order information inherent in $\langle z_1, z_2, ..., z_n\rangle$ is eliminated when it is represented as the *roots* of a complex polynomial. In other words, we apply the transformation, $\langle z_1, z_2, ...z_n\rangle \to \langle a_n, a_{n-1}, a_{n-2}, ..., a_0\rangle$ wherein $a_n, a_{n-1}, a_{n-2}, ...a_0 \in \mathbb{C}$ are the coefficients of the complex polynomial, $F(z) = a_nz^n + a_{n-1}z^{n-1} + ... + a_0$ whose roots lie at $z_1, z_2, ...z_n \in \mathbb{C}$. The immediate question then is, what is a *necessary* and *sufficient* set of constraints on $\langle a_n, a_{n-1}, a_{n-2}, ...a_0\rangle \in \mathbb{C}^{n+1}$ such that all roots of the polynomial $F(z) = a_nz^n + a_{n-1}z^{n-1} + ... + a_0$ lie on the unit circle, i.e., $\forall$ roots z_i, $|z_i| = 1$. We answer this question in two steps. First, we consider the case of distinct roots, and subsequently we consider the general case of distinct or multiple roots.

Theorem 1 *Let* $f(z) = a_nz^n + a_{n-1}z^{n-1} + ... + a_1z + a_0$ *be a complex polynomial of degree* n. *Let*

(i) $f^*(z)$ *be defined as* $f^*(z) = z^n\bar{f}(1/z) = \bar{a}_0z^n + \bar{a}_1z^{n-1} + ... + \bar{a}_n$.

(ii) $f'(z)$ *be the derivative of* $f(z)$.

(iii) The sequence $\langle f_0(z), f_1(z), ..., f_{n-1}(z)\rangle$ *be constructed as follows.*

- $f_j(z) = \sum_{k=0}^{n-1-j} b_k^{(j)}z^k$ *where*
- $f_0(z) = f'(z)$ *and*

[12] A Group G acts freely on a set X if $\forall x$ ($gx = x$ implies $g = e$).

– $f_{j+1}(z) = \bar{b}_0^{(j)} f_j(z) - b_{n-1-j}^{(j)} f_j^*(z), \quad j = 0, 1, ..., n-2.$

In each polynomial $f_j(z)$, the constant term $b_0^{(j)}$ is a real number which we denote by δ_j; namely, $\delta_{j+1} = b_0^{(j+1)} = |b_0^{(j)}|^2 - |b_{n-1-j}^{(j)}|^2$, $j = 0, 1, ..., n-2$.

Then, necessary *and* sufficient *conditions for all roots of $f(z)$ to be* **distinct** *and to lie on the unit circle, $|z| = 1$, assuming w.l.o.g that $a_n = 1$, are:*

(i) $|a_0| = 1$, *and* $a_i = \bar{a}_{n-i}.a_0, \quad$ *for* $i = 1, 2, ..., n-1$. *and*

(ii) $\delta_1 < 0$ *and* $\delta_j > 0 \quad$ *for* $j = 2, 3, ..., n-1$.

Proof: *Appendix: I.*

Stated informally, condition (i) of the above theorem ensures that the degree of freedom reflected in the dimensionality of the initial space does not change as a result of the transformation. In more specific terms, of the coefficients $\{a_{n-1}, a_{n-2}, ..., a_0\}$ (a_n=1 w.l.o.g), (1) a_0 has a degree of freedom one ($|a_0| = 1$) and (2) if n is odd, $\{a_{\lceil n/2 \rceil - 1}, ..., a_1\}$ can be computed directly from $\{a_{n-1}, ..., a_{\lceil n/2 \rceil}$, and $a_0\}$ or (3) if n is even, $a_{\lceil n/2 \rceil}$ has a degree of freedom one ($a_{\lceil n/2 \rceil} = \bar{a}_{\lceil n/2 \rceil}.a_0$ implies that $\angle a_{\lceil n/2 \rceil} = (1/2)\angle a_0$) and $\{a_{\lceil n/2 \rceil - 1}, ..., a_1\}$ can be computed directly from $\{a_{n-1}, ..., a_{\lceil n/2 \rceil + 1}$, and $a_0\}$.

In other words, if n is odd, the set $\{a_{n-1}, ..., a_{\lceil n/2 \rceil}; a_0\} \in \mathbb{C}^{\lfloor n/2 \rfloor} \times S^1$ completely specifies the complex polynomial in question, and if n is even, the set $\{a_{n-1}, ..., a_{\lceil n/2 \rceil + 1}; a_{\lceil n/2 \rceil}; a_0\} \in \mathbb{C}^{\lfloor n/2 \rfloor - 1} \times \mathbb{M}^2$ does the same. $\mathbb{M}^2$ denotes the 2-dimensional *Möbius* band and we shall presently demonstrate that $\langle a_{\lceil n/2 \rceil}, a_0 \rangle \in \mathbb{M}^2$ for the case where n is even.
We have already noted that when n is even,
(a) $|a_0| = 1$, and
(b) $\angle a_{\lceil n/2 \rceil} = (1/2)\angle a_0$.

While the obvious scheme would be to represent only $a_{\lceil n/2 \rceil} \in \mathbb{C}$ (a_0 being entirely specified in $|a_0| = 1$ and $\angle a_0 = 2.\angle a_{\lceil n/2 \rceil}$), problems arise when $|a_{\lceil n/2 \rceil}| = 0$, whereupon $\angle a_0$ becomes indeterminate. The alternative is to represent $\langle a_{\lceil n/2 \rceil}, a_0 \rangle$ as $\langle |a_{\lceil n/2 \rceil}|, \angle a_0 \rangle$. The problem with this approach is that $(1/2)\angle a_0$ has two solutions, θ and $(\theta + \pi)$ where $\theta \in [0, \pi)$. This problem can, however, be solved by setting the primary solution θ to represent the value of $(1/2)\angle a_0$, and by transferring $a_{\lceil n/2 \rceil}$'s choice between θ and $(\theta + \pi)$ to its modulus. (Positive $|a_{\lceil n/2 \rceil}|$ implies θ and negative $|a_{\lceil n/2 \rceil}|$ implies $(\theta + \pi)$). Then
(a) instead of $|a_{\lceil n/2 \rceil}| \in [0, +\infty)$, we have $\pm|a_{\lceil n/2 \rceil}| \in (-\infty, +\infty)$, and
(b) topological constraints require that all points $\langle |a_{\lceil n/2 \rceil}|, \angle a_0 \rangle \equiv \langle \alpha, 0 \rangle$ be identified with $\langle |a_{\lceil n/2 \rceil}|, \angle a_0 \rangle \equiv \langle -\alpha, 2\pi \rangle$.
Thus $\langle a_{\lceil n/2 \rceil}, a_0 \rangle \in \mathbb{M}^2$.

Condition (ii) of the above theorem enforces an additional set of $(n-1)$ constraints expressed in the form of *strict* inequalities on *continuous* functions over the transformed space ($\mathbb{C}^{\lfloor n/2 \rfloor} \times S^1$ or $\mathbb{C}^{\lfloor n/2 \rfloor - 1} \times \mathbb{M}^2$, as the case may be). That the functions are continuous is evident from their being composed of operators $+, \times$, and $\bar{}$. We note immediately, based on continuity and strict inequality, that the resulting space is *open* in $\mathbb{C}^{\lfloor n/2 \rfloor} \times S^1$ (n is odd) or $\mathbb{C}^{\lfloor n/2 \rfloor - 1} \times \mathbb{M}^2$ (n is even). We denote the resulting space by $\mathbb{L}_n$.

We now consider the general case wherein the polynomial is allowed to have both distinct and multiple roots.

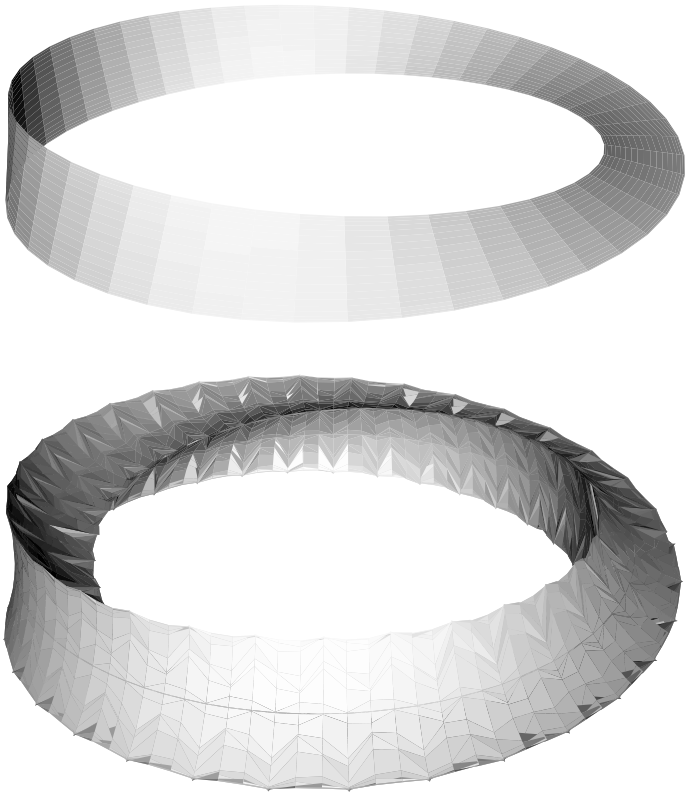

Figure 3: Phase spaces for n=2 and n=3.

Theorem 2 *Necessary and sufficient condition for all roots to lie on the unit circle,* $|z| = 1$*, without the constraint that they be distinct, i.e., when multiple roots are allowed, is the* **closure** *of* $\mathbb{L}_n$ *(*$\overline{\mathbb{L}_n}$*) in* $\mathbb{C}^{\lfloor n/2 \rfloor} \times S^1$ *(*n *is odd) or* $\mathbb{C}^{\lfloor n/2 \rfloor - 1} \times \mathbb{M}^2$ *(*n *is even).*

Proof: *Appendix: I.*

That the space is bounded is evident from the trivial bounds, $\forall i |a_i| \leq {}^nC_i$.

Corollary 1 *The transformed space is a* **compact** *manifold; a subset of the same dimension of* $\mathbb{C}^{\lfloor n/2 \rfloor} \times S^1$ *if* n *is* odd *or of* $\mathbb{C}^{\lfloor n/2 \rfloor - 1} \times \mathbb{M}^2$ *if* n *is* even.

The nature of the spaces corresponding to dimensions $n = 1, 2, 3...$ is best demonstrated in figures. For $n = 1$, the phase space is the unit circle S^1. For $n = 2$, it is the *Möbius* band, and for $n = 3$, it is a solid torus whose cross-section is a concave triangle that revolves around its centroid as one travels around the torus. Figure 3 presents the phase spaces for $n = 2$ and $n = 3$.

Finally, the phase space for the entire neuronal system is the Cartesian product of the phase spaces of individual neurons.

In the beginning of this section we noted that if a limited spike history of *all* neurons are recorded, as in the above description of the state of a neuronal system, $P^i(.)$ (the

superscript referring to neuron i) can be defined on an expanded space, namely,
$P^i(x_1^1, ...x_1^{n_1}, x_2^1, ...x_2^{n_2}, ...x_m^1...x_m^{n_m}; x_i^1, ...x_i^{n_i}) =$
$$P^i_{Afferent}(x_1^1, ...x_1^{n_1}, x_2^1, ...x_2^{n_2}, ...x_m^1...x_m^{n_m}) + P^i_{Refractory}(x_i^1, ...x_i^{n_i})$$

where $\langle x_j^1, ...x_j^{n_j}\rangle$ for $j = 1..m$ denote the spike records of neurons pre-synaptic to respective synapses on neuron i, and $\langle x_i^1, ...x_i^{n_i}\rangle$ denotes the spike record of neuron i itself. Both $P_{Afferent}(.)$ and $P_{Refractory}(.)$ were assumed to be C^1 functions and it must be verified that this remains the case on the transformed space. In Appendix: II we define function $\widetilde{P}^i : {}^1\overline{\mathbb{L}}_{n_1} \times {}^2\overline{\mathbb{L}}_{n_2} \times ... \times {}^m\overline{\mathbb{L}}_{n_m} \times {}^i\overline{\mathbb{L}}_{n_i} \to \mathbb{R}$ that satisfies this criterion.

The Velocity Field

We noted in the previous section that if $\mathcal{S}$ denotes the total number of neurons in the system, the resultant phase space is a compact subset of

$$\prod_{i=1}^{\mathcal{S}} (\mathbb{C}^{\lfloor n_i/2 \rfloor} \times S^1 | \mathbb{C}^{\lfloor n_i/2 \rfloor - 1} \times \mathbb{M}^2), \ namely, \ \prod_{i=1}^{\mathcal{S}} {}^i\overline{\mathbb{L}}_{n_i}$$

It follows immediately from the smoothness of the ambient manifolds and the compactness of the subsets in question that the specified space does inherit the tangent bundle of the ambient space without ambiguity. In this section we stipulate the velocity vector field, $\mathcal{V} : \prod_{i=1}^{\mathcal{S}} {}^i\overline{\mathbb{L}}_{n_i} \to \prod_{i=1}^{\mathcal{S}} T({}^i\overline{\mathbb{L}}_{n_i})$, that arises from the natural dynamics of the system. $T(.)$ here denotes the tangent bundle.

Informally, the natural dynamics of the system can be described as follows. Spikes corresponding to each neuron are partitioned into two sets; dead and live. Those spikes whose effectiveness on all post-synaptic neurons have expired, and are presently stationed at $x_j^i = 0 = 2\pi$, we denote as dead spikes. The rest we denote as live spikes. If the state of the system at a given instant is such that neither any live spike is on the verge of death nor is any neuron on the verge of spiking, then the dynamics stipulates that all *live* spikes continue to age uniformly. If a spike is on the verge of death, it simply expires, i.e., stops aging. This occurs precisely when a spike reaches $x_j^i = 0 = 2\pi$. If a neuron is on the verge of spiking based on previously discussed criteria, exactly one dead spike corresponding to that neuron is turned live. We impose a vector field on the transformed space that, in essence, reflects this dynamics.

Formally, we denote by $p \in \langle {}^1\overline{\mathbb{L}}_{n_1} \times {}^2\overline{\mathbb{L}}_{n_2} \times ... \times {}^{\mathcal{S}}\overline{\mathbb{L}}_{n_{\mathcal{S}}}\rangle$ a point in the phase space, and by $\langle p_1, p_2, ...p_{\mathcal{S}}\rangle$ its projection on the corresponding individual spaces, i.e., $p_i \in {}^i\overline{\mathbb{L}}_{n_i}$. Given any such $p = \langle p_1, p_2, ...p_{\mathcal{S}}\rangle$ we first present an analytic characterization of the number of dead spikes corresponding to each neuron, and subsequently relate it to the *geometric structure* of any individual phase space ${}^i\overline{\mathbb{L}}_{n_i}$.

Let σ_i denote the number of dead spikes corresponding to neuron i which at a given instant is in state $\langle a_{n-1}, ..., a_{\lceil n/2 \rceil}; \angle a_0\rangle = p_i \in {}^i\overline{\mathbb{L}}_{n_i}$. We consider the corresponding complex polynomial, $f(z) = z^n + a_{n-1}z^{n-1} + ... + a_{\lceil n/2 \rceil}z^{\lceil n/2 \rceil} + ... + \bar{a}_{n-1}a_0 z + a_0$ and note that

(1) If $f(1) = f^0(1) = 0$, and $f'(1) = f^1(1) = 0$, and ... $f^{n-1}(1) = 0$, then $\sigma = n$. Else
(2) If $f^0(1) = 0$, and $f^1(1) = 0$, and ... $f^{n-2}(1) = 0$, then $\sigma = n - 1$. Else
$\vdots$

(n-1) If $f^0(1) = 0$, then $\sigma = 1$. Else
(n) $\sigma = 0$.

Each such $f^i(z)$ is a *smooth* function, and consequently, the sub-spaces corresponding to $\sigma = 1, 2, ...n$ are smooth structures. We now consider what such a characterization entails in terms of the geometric structure of the phase spaces of individual neurons.

To begin with, we note that $Space|_{\sigma \geq i} \subset Space|_{\sigma \geq i-1}$. In the previous section we established that the phase space of a neuron with a sum total of k spikes is a k *dimensional* compact manifold. We now compare (a) a phase space A corresponding to k spikes with (b) the subset $\sigma \geq 1$ of a phase space B corresponding to $(k+1)$ spikes. Equating the appropriate polynomials, $(z-1)[z^n + a_{n-1}z^{n-1} + ... + a_0] = z^{n+1} + b_n z^n + ... + b_0$, we get

$$\begin{array}{lll} b_n = a_{n-1} - 1 & or, & a_{n-1} = b_n + 1 \\ b_{n-1} = a_{n-2} - a_{n-1} & or, & a_{n-2} = b_{n-1} + b_n + 1 \\ \vdots & \vdots & \vdots \\ b_1 = a_0 - a_1 & or, & a_0 = b_1 + b_2 + ...b_n + 1 \\ b_0 = -a_0 & satisfying, & 1 + b_n + b_{n-1} + ...b_0 = 0 \end{array}$$

We show that the mapping $F : A \rightarrow B$, $F\langle a_{n-1}, ..., a_{\lceil n/2 \rceil}; \angle a_0 \rangle = \langle b_n, ..., b_{\lceil (n+1)/2 \rceil}; \angle b_0 \rangle$, is a one-to-one *immersion*, and based on the previously demonstrated compactness of A, also an *imbedding*. Furthermore, repeated application of the argument establishes that $\forall i \; Space|_{\sigma \geq i}$ is a compact *regular-submanifold/ imbedding/ one-to-one immersion* of codimension 1 of $Space|_{\sigma \geq i-1}$.

That the mapping is one-to-one is obvious from the above set of equations. That it is an immersion, i.e., that *rank* F = *dim* A at all points, follows from the description of (DF) which when simplified can be represented as the $(n+1 \times n)$ matrix

$$\left(\begin{array}{cc} I & 0 \\ 0 & C \end{array} \right) \; for \; dim \; A = even, \; and \left(\begin{array}{c} I \\ D \end{array} \right) \; for \; dim \; A = odd.$$

where I is the identity matrix of appropriate dimension, C is $\langle \cos(\frac{\angle a_0}{2}), \sin(\frac{\angle a_0}{2}) \rangle^T$, D is $\langle \cos(\frac{\angle a_0}{2}) \Re a_{\lceil n/2 \rceil} + \sin(\frac{\angle a_0}{2}) \Im a_{\lceil n/2 \rceil}, 0, 0, ..., 2\sin(\frac{\angle a_0}{2}), -2\cos(\frac{\angle a_0}{2}) \rangle$, and 0 is the zero matrix of appropriate dimension.

Figure 4 displays the subspace $\sigma \geq 1$ located within the phase space corresponding to $n = 3$ (imbedding of a *Möbius* band). The torus is cut in half, and the *Möbius* band within each half is exposed separately. The subspace $\sigma \geq 2$ (imbedding of a circle), which is not shown here, lies on the *Möbius* band, drifting to the border of the band on the right of the figure (to the extreme right on the right side), and back to the center of the band on the left of the figure.

We denote by ${}^i\overline{\mathbb{L}}^j_{n_i}$ the subspace $\sigma \geq j$ for neuron i. Consequently, we have, ${}^i\overline{\mathbb{L}}_{n_i} = {}^i\overline{\mathbb{L}}^0_{n_i} \supset {}^i\overline{\mathbb{L}}^1_{n_i} \supset ... \supset {}^i\overline{\mathbb{L}}^{n_i}_{n_i}$ for the n_i-dimensional manifold ${}^i\overline{\mathbb{L}}_{n_i}$.

It must be noted that the function $F : A \rightarrow B$ not only maps phase spaces but also maps flows identically; a fact manifest in the informal description of the dynamics of the system.[13] This has the important ramification that the total number of spikes assigned to

[13]Only live spikes age uniformly. All dead spikes, how many ever there are, remain stationary at $e^{i0} = 1$ and therefore register as a constant factor in the dynamics of the neuron.

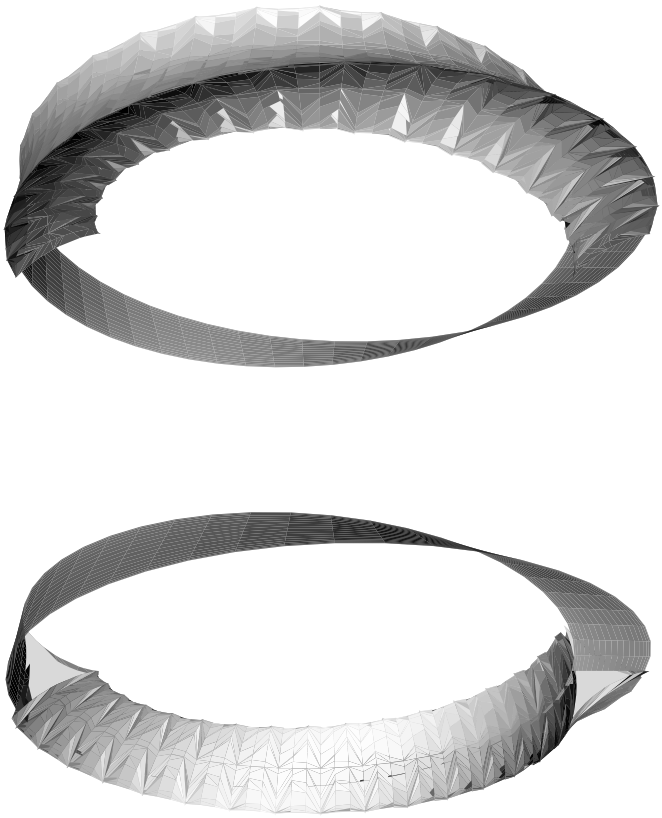

Figure 4: Subspace $\sigma \geq 1$ in the phase space for n=3.

a neuron has little impact on its phase space dynamics. $F : A \rightarrow B$, in essence, constitutes a bridge between all flows that correspond to a given number of *live* spike possessed by a neuron over a given interval of time. While the total number of spikes assigned to a neuron dictates the dimensionality of its entire phase space, flows corresponding to a given number of *live* spikes lie on a fixed dimensional sub-manifold and are C^{∞}-*conjugate* to each other. [14] For example, all flows corresponding to two live spikes are C^{∞}-*conjugate* to flows on the *Möbius* band irrespective of the dimensionality of the ambient phase space, and so on.

We now refer to the standard definition of a k-dimensional C^p *hyper-surface* in an m-dimensional manifold, namely, $S \subset M$ is a k-dimensional C^p *hyper-surface* if for every point $s \in S$, there exists a co-ordinate neighborhood $\langle U, \phi \rangle$ of M that contains s such that $\phi(U \cap S)$ is the *image* of an open set in $\mathbb{R}^k$ under an *injective* C^p diffeomorphism, $\varphi : \mathbb{R}^k \rightarrow \mathbb{R}^m$.

It follows immediately from the definition that $\forall j > 0$ ${}^i\overline{\mathbb{L}}^j_{n_i} \subset {}^i\overline{\mathbb{L}}^0_{n_i}$ is a C^{∞} hyper-surface of dimension $n_i - j$.

In the previous section we defined a C^1 function, $\widetilde{P}^i : {}^1\overline{\mathbb{L}}_{n_1} \times {}^2\overline{\mathbb{L}}_{n_2} \times ... \times {}^m\overline{\mathbb{L}}_{n_m} \times {}^i\overline{\mathbb{L}}_{n_i} \rightarrow \mathbb{R}$ for the potential at the soma of neuron i. We denote by P^S_i the subset of the space wherein $\widetilde{P}^i(.) = T$, and by P^I_i the subset wherein $\widetilde{P}^i(.) = T$ and $d\widetilde{P}^i(.)/dt \geq 0$. Trivially then, $P^I_i \subseteq P^S_i$. Based on the implicit function theorem and the fact that at all points satisfying

[14] The mapping $F : A \rightarrow B$ is C^{∞}.

$\widetilde{P}^i(.) = T \; \exists \; direction \; x$ such that $\partial \widetilde{P}^i(.)/\partial x \neq 0$[15], it follows that P_i^S is a C^1 hyper-surface (a C^1 regular sub-manifold of codimension 1). Moreover, since $\widetilde{P}^i(.)$ is a C^1 function, $d\widetilde{P}^i(.)/dt$ along any direction d/dt is continuous on P_i^S, and it therefore follows that P_i^I is a closed subset of P_i^S.

To summarize, the phase space $\langle {}^1\overline{\mathbb{L}}_{n_1} \times {}^2\overline{\mathbb{L}}_{n_2} \times ... \times {}^{\mathcal{S}}\overline{\mathbb{L}}_{n_{\mathcal{S}}} \rangle$ contains the following significant structural elements.

1 $\mathcal{S}$ C^1 hyper-surfaces P_i^I for $i = 1..\mathcal{S}$. Each such surface identifies the subset of the entire phase space that induces the corresponding neuron to spike.

2 For each ${}^i\overline{\mathbb{L}}_{n_i}$, C^∞ hyper-surfaces ${}^i\overline{\mathbb{L}}^1_{n_i} \supset {}^i\overline{\mathbb{L}}^2_{n_i} \supset ... \supset {}^i\overline{\mathbb{L}}^{n_i}_{n_i}$ of successively lower dimensions. Each such surface identifies the subset of the individual neuron's phase space that corresponds to a fixed number of dead (and therefore live) spikes.

In the previous section we noted that $\overline{\mathbb{L}}_n$ is a subset (of same dimension) of $\mathbb{C}^{\lfloor n/2 \rfloor} \times S^1$ or $\mathbb{C}^{\lfloor n/2 \rfloor - 1} \times \mathbb{M}^2$ depending upon whether n is even or odd. We define a basis for $T_p(\overline{\mathbb{L}}_n)$ as follows.

- $\mathbb{C}$ is covered by a single co-ordinate neighborhood (U, ϕ) with $\phi(U) = \mathbb{R}^2$, $\phi(z) = \langle \Re z, \Im z \rangle$. The basis vectors are $\phi_*^{-1}(\partial/\partial x_1)$ (along $\Re z$) denoted by $\hat{a}_1$, and $\phi_*^{-1}(\partial/\partial x_2)$ (along $\Im z$) denoted by $\hat{a}_2$.[16]

  A C^∞-compatible co-ordinate neighborhood (V, ψ) with $V = \mathbb{C} - \{z | \Re z \geq 0, \Im z = 0\}$, $\psi(V) = \{(r, \theta) | r > 0, 0 < \theta < 2\pi\}$ is also retained for description in terms of radial co-ordinates. The corresponding basis vectors are, $\psi_*^{-1}(\partial/\partial r)$ denoted by $\hat{r}$, and $\psi_*^{-1}(\partial/\partial \theta)$ denoted by $\hat{\theta}$.

- S^1 is covered by two co-ordinate neighborhoods (U_1, ϕ_1) and (U_2, ϕ_2) with $U_1 = \{\angle a_0 \in S^1 | \angle a_0 \neq 0\}$, $\phi_1 : U_1 \rightarrow (0, 2\pi)$, and $U_2 = \{\angle a_0 \in S^1 | \angle a_0 \neq \pi\}$, $\phi_2 : U_2 \rightarrow (-\pi, \pi)$. The basis vector in the corresponding co-ordinate neighborhoods (U_1, ϕ_1) and (U_2, ϕ_2) are, ${\phi_1}_*^{-1}(d/d\theta)$ and ${\phi_2}_*^{-1}(d/d\theta)$. For arbitrary $\{\angle a_0 \in S^1 | \angle a_0 \neq 0, \pi\}$ they relate according to ${\phi_1}_*^{-1}(d/d\theta) = {\phi_2}_*^{-1}(d/d\theta)$. The basis vector can therefore be denoted unambiguously by $\hat{\theta}$.

- $\mathbb{M}^2$ is covered by two co-ordinate neighborhoods (U_1, ϕ_1) and (U_2, ϕ_2) with $U_1 = \{\langle \pm |a_{\lceil n/2 \rceil}|, \angle a_0 \rangle \in \mathbb{M}^2 | \angle a_0 \neq 0\}$, $\phi_1 : U_1 \rightarrow \{\mathbb{R} \times (0, 2\pi)\}$, and $U_2 = \{\langle \pm |a_{\lceil n/2 \rceil}|, \angle a_0 \rangle \in \mathbb{M}^2 | \angle a_0 \neq \pi\}$, $\phi_2 : U_2 \rightarrow \{\mathbb{R} \times (-\pi, \pi)\}$.[17] The basis vectors in the corresponding co-ordinate neighborhoods (U_1, ϕ_1) and (U_2, ϕ_2) along respective directions $\pm |a_{\lceil n/2 \rceil}|$ and $\angle a_0$ are, $\langle {\phi_1}_*^{-1}(\partial/\partial x_1), {\phi_1}_*^{-1}(\partial/\partial x_2) \rangle$ and $\langle {\phi_2}_*^{-1}(\partial/\partial x_1), {\phi_2}_*^{-1}(\partial/\partial x_2) \rangle$. For arbitrary $\{\langle \pm |a_{\lceil n/2 \rceil}|, \angle a_0 \rangle \in \mathbb{M}^2 | \angle a_0 \in (0, \pi)\}$ they relate according to ${\phi_1}_*^{-1}(\partial/\partial x_1) = {\phi_2}_*^{-1}(\partial/\partial x_1)$ and ${\phi_1}_*^{-1}(\partial/\partial x_2) = {\phi_2}_*^{-1}(\partial/\partial x_2)$ and for arbitrary $\{\langle \pm |a_{\lceil n/2 \rceil}|, \angle a_0 \rangle \in \mathbb{M}^2 | \angle a_0 \in (\pi, 2\pi) \equiv (-\pi, 0)\}$ they relate according to ${\phi_1}_*^{-1}(\partial/\partial x_1) = -{\phi_2}_*^{-1}(\partial/\partial x_1)$

[15] This is not the case only in the trivial instance where the subset $\widetilde{P}^i(.) = T$ is a single point.In all other cases there exist effective spikes that satisfy the above criterion.

[16] We use the notation, $F_*(X_p)f = X_p(f \circ F)$ where F is a C^∞ map of manifolds, X_p is a tangent vector at p, and f is an arbitrary function belonging to $C^\infty(p)$.

[17] In $\phi_1(U_1)$ the primary solution $(1/2)\angle a_0$ is the one that lies in $(0, \pi)$ and in $\phi_2(U_2)$ the primary solution $(1/2)\angle a_0$ is the one that lies in $(-\pi/2, \pi/2)$.

and $\phi_{1_*}^{-1}(\partial/\partial x_2) = \phi_{2_*}^{-1}(\partial/\partial x_2)$. The basis vectors are denoted by $\hat{c}_1 = \phi_{1_*}^{-1}(\partial/\partial x_1)$ in U_1 and $\hat{c}_2 = \phi_{2_*}^{-1}(\partial/\partial x_1)$ in U_2 (along $\pm|a_{\lceil n/2\rceil}|$), and $\hat{\theta} = \phi_{1_*}^{-1}(\partial/\partial x_2) = \phi_{2_*}^{-1}(\partial/\partial x_2)$ in $U_1 \cup U_2 = \mathbb{M}^2$ (along $\angle a_0$).

We now define the vector field by stipulating two functions, $\mathcal{V}^1 : \prod_{i=1}^{\mathcal{S}} {}^i\overline{\mathbb{L}}_{n_i} \rightarrow \prod_{i=1}^{\mathcal{S}} T({}^i\overline{\mathbb{L}}_{n_i})$ for the case wherein $p \in \prod_{i=1}^{\mathcal{S}} {}^i\overline{\mathbb{L}}_{n_i}$ does not lie on any P_i^I, and $\mathcal{V}^2 : \prod_{i=1}^{\mathcal{S}} {}^i\overline{\mathbb{L}}_{n_i} \rightarrow \prod_{i=1}^{\mathcal{S}} T({}^i\overline{\mathbb{L}}_{n_i})$ for the case wherein it does.

It is clear from the informal description of the natural dynamics of the system that given $p = \langle p_1, p_2, ...p_{\mathcal{S}}\rangle$, $p_i \in {}^i\overline{\mathbb{L}}_{n_i}$, $\mathcal{V}^1(p) = \frac{dp}{dt} = \langle \frac{dp_1}{dt}, \frac{dp_2}{dt}, ..., \frac{dp_{\mathcal{S}}}{dt}\rangle = \langle \mathcal{V}_1^1(p), \mathcal{V}_2^1(p), ..., \mathcal{V}_{\mathcal{S}}^1(p)\rangle$ can be defined as $\langle \mathcal{V}_1^1(p_1), \mathcal{V}_2^1(p_2), ..., \mathcal{V}_{\mathcal{S}}^1(p_{\mathcal{S}})\rangle$. That is to say that each component $\mathcal{V}_i^1$ of $\mathcal{V}^1$ is solely a function of $p_i \in {}^i\overline{\mathbb{L}}_{n_i}$. This is also true for $\mathcal{V}^2$; once it is determined which if any P_i^I's the point p lies on, each component can be computed based solely on p_i.

We define $\mathcal{V}_i^1\langle a_{n-1}, ..., a_{\lceil n/2\rceil}; \angle a_0; \sigma(a_{n-1}, ..., a_{\lceil n/2\rceil}; \angle a_0)\rangle$ (σ denotes the number of dead spikes computed as above) for arbitrary i as follows.

Let point p_i represent the polynomial $z^n + a_{n-1}z^{n-1} + ... + a_0 = \prod_{i=1}^{n}(z - z_i)$. Of the n roots, $\langle z_1, z_2, ...z_n\rangle$, σ are stationary at $z_i = 1$ (or $dz_i/dt = 0$), and the rest rotate at constant speed, i.e., $z_i = e^{i(\theta_i + \frac{2\pi t}{\Upsilon})}$ (or $dz_i/dt = \frac{2\pi i}{\Upsilon} z_i$). We first define the dynamics in the ambient Euclidean space, i.e., assuming that $\langle a_{n-1}, ..., a_{\lceil n/2\rceil}; a_0\rangle \in \mathbb{C}^{\lfloor n/2\rfloor+1}$.

Theorem 3 *If* $p_i = \langle a_{n-1}, ..., a_{\lceil n/2\rceil}; a_0\rangle \in \mathbb{C}^{\lfloor n/2\rfloor+1}$, *then* $\dfrac{dp_i}{dt}$ *is given by*

i) $\dfrac{da_0}{dt} = \dfrac{2\pi i}{\Upsilon}(n - \sigma)a_0$,

ii) $\dfrac{da_{n-k}}{dt} = \dfrac{2\pi i}{\Upsilon}[k(a_{n-k} - (-1)^k.\ {}^{\sigma}C_k) + \sigma\sum_{j=1}^{k-1}(a_{n-j} - (-1)^j.\ {}^{\sigma}C_j)]$, *and*

iii) For n=even, $\dfrac{d|a_{n/2}|}{dt} = \dfrac{2\pi i\sigma}{\Upsilon\sqrt{a_0}}[\sum_{j=0}^{\frac{n}{2}-1} a_{n-j} + \dfrac{a_{n/2}}{2}]$

where $\sqrt{a_0}$ *represents the primary root of* a_0, *and* $a_n = 1$.

Proof: *Appendix: III.*

Corollary 2 *In local co-ordinates,* $\mathcal{V}_i^1(p_i) : {}^i\overline{\mathbb{L}}_{n_i} \rightarrow T_{p_i}({}^i\overline{\mathbb{L}}_{n_i})$ *is defined as*

i) $\dfrac{d\angle a_0}{dt} = \dfrac{2\pi}{\Upsilon}(n - \sigma)\hat{\theta}$,

ii) If the value of $\dfrac{da_{n-k}}{dt}$ *(for* k *such that* $1 \leq k \leq \lfloor\frac{n}{2}\rfloor$*) defined above is denoted by* $X \in \mathbb{C}$, *then* $\dfrac{da_{n-k}}{dt} = \Re X\hat{a}_1 + \Im X\hat{a}_2$, *and*

iii) For n=even, $\dfrac{d|a_{n/2}|}{dt} = \dfrac{2\pi i\sigma}{\Upsilon}[e^{-i\frac{\angle a_0}{2}}\sum_{j=0}^{\frac{n}{2}-1} a_{n-j} + \dfrac{|a_{n/2}|}{2}]\hat{c}_1$ *or* $\hat{c}_2$ *(*$\hat{c}_1$ *when* $p_i \in U_1 \subset \mathbb{M}^2$, *in which case* $\dfrac{\angle a_0}{2} \in (0, \pi)$, *and* $\hat{c}_2$ *when* $p \in U_2 \subset \mathbb{M}^2$, *in which case* $\dfrac{\angle a_0}{2} \in (-\pi/2, \pi/2)$*).*

As noted earlier, flows corresponding to the vector field $\mathcal{V}_i^1$ on $({}^i\overline{\mathbb{L}}_{n_i}^{\sigma} - {}^i\overline{\mathbb{L}}_{n_i}^{\sigma+1})$ (the sub-manifold of ${}^i\overline{\mathbb{L}}_{n_i}$ that corresponds to exactly $(n_i - \sigma)$ *live* spikes) are C^{∞}-*conjugate* to flows on the manifold $(\overline{\mathbb{L}}_{(n_i-\sigma)}^0 - \overline{\mathbb{L}}_{(n_i-\sigma)}^1)$ of dimension $(n_i - \sigma)$ with *no* dead spikes.

It is therefore worthwhile to consider the form that $\mathcal{V}_i^1$ takes on $(\overline{\mathbb{L}}^0_{(n_i-\sigma)} - \overline{\mathbb{L}}^1_{(n_i-\sigma)})$. Here of course, $p_i \in \overline{\mathbb{L}}_{(n_i-\sigma)}$ is represented as $p_i = \langle a_{n_i-\sigma-1}, ..., a_{\lceil (n_i-\sigma)/2 \rceil}; a_0 \rangle$. It follows immediately (setting $n := (n-\sigma)$ and $\sigma := 0$) from the above theorem that

Corollary 3 *$\mathcal{V}_i^1$ for the corresponding C^∞-conjugate flows on $(\overline{\mathbb{L}}^0_{(n_i-\sigma)} - \overline{\mathbb{L}}^1_{(n_i-\sigma)})$ is given by*
i) $\dfrac{da_0}{dt} = \dfrac{2\pi}{\Upsilon}(n-\sigma)\hat{\theta}$,
ii) $\forall k$ *such that* $(1 \leq k \leq \lfloor \frac{n-\sigma}{2} \rfloor)$, $\dfrac{da_{n-\sigma-k}}{dt} = \dfrac{2\pi}{\Upsilon} k\hat{\theta}$, *and*
iii) For the case wherein $(n-\sigma)$ *is even,* $\dfrac{d|a_{(n-\sigma)/2}|}{dt} = 0$.

In other words, each parameter revolves around its origin at uniform speed. Furthermore, the speed increases in discrete steps of $(2\pi/\Upsilon)$ for successive parameters.

We now turn our attention to $\mathcal{V}^2(p)$. It is clear that while $2^{\mathcal{S}}$ separate versions of $\mathcal{V}^2$ need to be defined, one for each of $p \in 2^{(P_1^I, P_2^I, ..., P_{\mathcal{S}}^I)}$, each such version is an element of $\prod_{i=1}^{\mathcal{S}} \mathcal{V}_i^1(p_i)|\mathcal{V}_i^2(p_i)$ wherein $\mathcal{V}_i^2(p_i)$ represents the projection of $\mathcal{V}(p)$ on $T_{p_i}({}^i\overline{\mathbb{L}}_{n_i})$ when $p \in P_i^I$.

Proceeding with the definition of $\mathcal{V}_i^2(p_i) : {}^i\overline{\mathbb{L}}_{n_i} \rightarrow T_{p_i}({}^i\overline{\mathbb{L}}_{n_i})$, we note immediately that $\mathcal{V}_i^2(p_i)$ can be obtained from $\mathcal{V}_i^1(p_i)$ by setting σ to $(\sigma - 1)$. In other words, $\mathcal{V}_i^2(p_i)$ for $p_i \in ({}^i\overline{\mathbb{L}}^{\sigma}_{n_i} - {}^i\overline{\mathbb{L}}^{\sigma+1}_{n_i})$ is equivalent to $\mathcal{V}_i^1(p_i)$ on ${}^i\overline{\mathbb{L}}^{\sigma-1}_{n_i}$ *ignoring* the fact that p_i lies additionally on ${}^i\overline{\mathbb{L}}^{\sigma}_{n_i} \subset {}^i\overline{\mathbb{L}}^{\sigma-1}_{n_i}$.

It is clear that the field $\mathcal{V} : \prod_{i=1}^{\mathcal{S}} {}^i\overline{\mathbb{L}}_{n_i} \rightarrow \prod_{i=1}^{\mathcal{S}} T({}^i\overline{\mathbb{L}}_{n_i})$ just defined is *discontinuous*. It must, therefore, be confirmed that not only is the vector field consistent with previous characterization of the dynamics of the system, but also that there is a differential equation theory that maps the field to the natural dynamics of the physical system. The rest of this section is devoted to the question of consistency and the appropriate differential equation theory for discontinuous right-hand-side is presented in Appendix: III.

To summarize, two discontinuous fields $\mathcal{V}_i^1(p_i)$ and $\mathcal{V}_i^2(p_i)$ have been defined on each individual space ${}^i\overline{\mathbb{L}}_{n_i}$. $\mathcal{V}(p)$ is defined as $\prod_{i=1}^{\mathcal{S}} \mathcal{V}_i^1(p_i)|\mathcal{V}_i^2(p_i)$, the choice between $\mathcal{V}_i^1$ and $\mathcal{V}_i^2$ determined by whether $p = \langle p_1, p_2 ..., p_{\mathcal{S}} \rangle$ does or does not lie on P_i^I. Both $\mathcal{V}_i^1$ and $\mathcal{V}_i^2$ are, however, smooth on $({}^i\overline{\mathbb{L}}^{\sigma}_{n_i} - {}^i\overline{\mathbb{L}}^{\sigma+1}_{n_i})$ for any σ, which in conjunction with the stipulation[18] that the projection of a trajectory $\Psi(\mathbf{x}, t)$ on ${}^i\overline{\mathbb{L}}^{\sigma}_{n_i}$ remains on it unless (a) it meets ${}^i\overline{\mathbb{L}}^{\sigma+1}_{n_i}$ or (b) it meets P_i^I, demonstrates that the only points where any trajectory is not differentiable are at (a) and (b).

This gives rise to the potential problem that $d\widetilde{P}^i(.)/dt$ might not be computable on P_i^I, for whereas $\widetilde{P}^i(.)$ is C^1, one component of $d\Psi(\mathbf{x}, t)/dt$ in ${}^i\overline{\mathbb{L}}_{n_i}$, namely, the velocity of the dead spike that just turned live, is undefined. However, one only needs to recall from Appendix: II that for any spike x stationed at e^{i0}, $\partial\widetilde{P}^i(.)/\partial x = 0$ over an infinitesimal interval $(e^{i\delta} > e^{ix} > e^{i(2\pi-\delta)})$. The problem is therefore resolved trivially.

Finally, the assumption that multiple roots (coincident spikes) occur only at e^{i0} (when the spikes are dead) can be enforced by requiring that all trajectories have only point intersections with P_i^I $\forall i$. The problematic region therefore, is $\{x \in P_i^I | d\widetilde{P}^i(.)/dt|_x = 0\}$, i.e., the part of the hyper-surface P_i^I that lies parallel to the velocity vector field. In this case it can be

[18] Derived from the natural dynamics of the system.

additionally required that a spike be generated only at first contact with P_i^I. In any case, the entire exercise amounts to choosing an appropriate subset of P_i^S, denoted by P_i^I, that signifies the region where neuron i spikes.

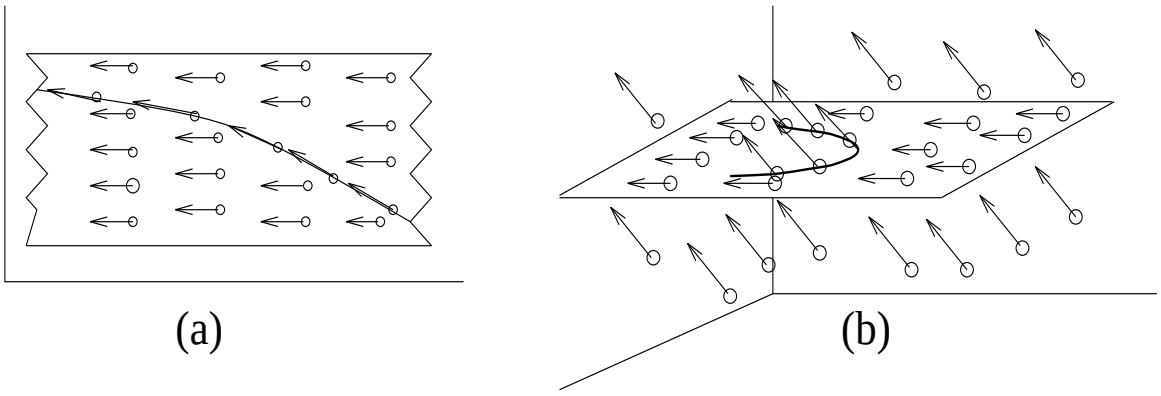

Figure 5: A schematic depiction of the vector field $\mathcal{V}$.

Figure 5 presents a schematic depiction of the vector field $\mathcal{V}$ described above. 5(a) displays the vector field corresponding to a patch of ${}^i\overline{\mathbb{L}}_1$ within a patch of ${}^i\overline{\mathbb{L}}_2$, and 5(b) displays the vector field corresponding to a P_i^I lying on a patch of ${}^i\overline{\mathbb{L}}_2$ within ${}^i\overline{\mathbb{L}}_3$.

4 Model Simulation and Results

As was pointed out in section 1, a model is worthwhile only to the extent to which it succeeds in emulating the salient behavior of the physical system it models. To this end we first investigate by means of simulation, the dynamical behavior of our model of a neuronal system. We shall demonstrate in this section that the *qualitative* aspects of the dynamics of our model instantiated suitably to meet anatomical specifications, are consistent with those of real neuronal systems as reported in numerous neurophysiological studies.

Before we can discuss the specifics of the experimental setup, we must establish a framework for comparison. A choice has to be made regarding the location in the brain and the size of the network of neurons to which the model is eventually compared. Furthermore, the issue of the level of detail at which the dynamical behavior of the neuronal system is to be regarded, must be resolved.

While in theory the entire brain can be viewed as an enormous network of neurons, such an outlook is neither practical nor particularly revealing. There is ample evidence indicating the presence of structure in the brain at all levels of detail. At the coarsest level, there are functionally distinct subsystems with neuronal pathways that link them. Each such subsystem exhibits distinctive connectivity patterns. The above approach to viewing the entire brain as an enormous network of neurons is unlikely to result in useful observation about the brain, any more than finite state assumptions help understand large but finite computer systems.

The cerebral cortex has been the subject of numerous physiological and anatomical investigations. As a result, extensive information is available about its composition (Braitenberg and Schüz 1991). The layered structure of the cortex ranks among the best documented and

least disputed characteristics of the cortex. The anatomically distinct neurons, home to each layer, have also been cataloged. Finally, there is a fair amount of evidence pointing towards columnar organization in the cortex (Mountcastle 1957; Hubel and Wiesel 1965). While not sharply defined everywhere, columns in general have a diameter of the order of 0.5 mm and contain $\approx 10^5$ neurons (Braitenberg 1978). Intra-column connectivity is markedly denser than inter-column connectivity. Whereas inhibitory connections play a significant role within a column, inter-column connections are distinctly excitatory. In the visual areas neurons within the same column even seem to share a common functional modality.

We have chosen as our target unit a neuronal system of the size of a column in the cerebral cortex. What confers to the unit its identity is the strong interactivity between its constituent neurons. Our view of a higher level subsystem (for example, an area in the visual cortex) is a collection of such units that are relatively weakly interactive.

4.1 Anatomical and Electro-Physiological Characteristics of Cortical Columns

As noted above, a column in the cortex contains $\approx 10^5$ neurons. The number of synapses each neuron makes ranges between 10^3 and 10^4. Based on quantification of the number of post-synaptic neighbors of pyramidal cells (Braitenberg 1978), it can be assumed that the probability of a neuron making *multiple* synapses on the dendrite of a post-synaptic neuron is fairly low. In other words, neurons distribute their synapses onto thousands of other neurons, and in turn receive their synapses from thousands of other neurons. The connectivity between neurons within a column has been experimentally ascertained to be *random* (Schüz 1992). Furthermore, the distribution of synapses on the collaterals of the neurons has also been identified as random (Braitenberg and Schüz 1991).

The neurons in the cerebral cortex can be divided into two main groups, the pyramidal and the non-pyramidal cells. Pyramidal cells make both local and long-range connections. They receive only Type II synapses (inhibitory) on their cell bodies and both Type I and Type II synapses on their dendrites. They are pre-synaptic to only Type I synapses (excitatory). Non-pyramidal cells do not make long-range connections. They receive both Type I and Type II synapses on their cell bodies and are presynaptically engaged in Type II synapses only (Peters and Proskauer 1980). Approximately 85% of all neurons in the cortex are pyramidal and the rest are non-pyramidal. Both kinds contribute on average to the same number of synapses per neuron.

The lengths of the axonal ramifications of pyramidal neurons in layers 2/3 range between 100 μm and 400 μm. The same is also true for most non-pyramidal neurons. The speed of propagation of an action potential can be estimated at $\approx 1\ m/s$ based on the fact that axons within a column are unmyelinated. Synaptic delays (time taken by a potential to cross a synapse) range between 0.3 $msec$ and 0.5 $msec$. Consequently, the time interval between the generation of an action potential at the axon-hillock of a pre-synaptic neuron and its subsequent arrival across the synapse of a post-synaptic neuron can be estimated to lie between 0.4 $msec$ and 0.9 $msec$.

Synapses on pyramidal neurons can be divided into four major categories: among excitatory synapses, those activating a non-$NMDA$ conductance and those activating a non-

$NMDA$ conductance in conjunction with a voltage dependent $NMDA$ conductance, and among inhibitory synapses, those utilizing the neuro-transmitter $GABA_A$ and those utilizing $GABA_B$. Non-$NMDA$ (excitatory) synapses are fast with response times of the order of 20 $msec$. $GABA_A$ (medium) and $GABA_B$ (slow) inhibitory synapses have response times of $\approx$ 80 $msec$ and $\approx$ 150 $msec$ respectively. Voltage dependent $NMDA$ conductance is much slower ($\approx$ 200 $msec$). The predominant view is that $GABA_A$ and $GABA_B$ synapses are present in approximately equal numbers and so are $NMDA$ and non-$NMDA$ synapses. Finally, anatomical investigations suggest that dendritic collaterals are seldom longer than $2-3$ space constants.[19]

The past few decades have witnessed numerous investigations into the electro-physiological activity of the cortex. Most of these studies fall under two major categories. The first is the recording of action potentials (spikes) which reflect the output of single cortical neurons with a time resolution of milliseconds (Abeles 1982, Krüger 1983), and the second is the recording of the Electroencephalogram (EEG), a slow continuous wave that reflects the activity of thousands of neurons (Grevins and Shaffer 1980, Jasper 1981).

One aspect that appears to be shared universally amongst single cortical neuron recordings is the apparent stochastic nature of the spike trains. In other words, the activity of cortical neurons seem to be *random*. We refer the reader to (Evarts 1964) for a recording of the spike train from a pyramidal tract cell of a monkey while it was awake, as well as while it was asleep. The recording is representative of what is generally observed in the case of spike train recordings of cortical neurons. Such observations have led many researchers to propose stochastic models for the neuron (MacGregor and Lewis 1977, Ricciardi 1977, Sampath and Srinivasan 1977). Recently however, (Softky and Koch 1992) have pointed out a fundamental contradiction between the large inter-spike variability observed in recordings and the much lower values predicted by well accepted stochastic biophysical models of the neuron.

In the case of EEG recordings the outputs are significantly more abstruse. Until the early eighties such recordings were regarded as little more than noise. Only recently have researchers come to regard the spontaneous oscillations of electrical activity manifest in the EEG recordings as the chaotic output of a nonlinear system (Basar 1990). Based on such assumptions several researchers have attempted to measure the dimensionality of various components of the EEG recordings (Babloyantz Nicolis and Salazar 1985; Röschke and Basar 1989). Unfortunately, the results remain varied and inconclusive.

4.2 Experimental Setup

We conducted simulation experiments to compare the dynamical behavior of our model to that of the actual physical system. Our purpose was to determine whether the *qualitative* characteristics of the data generated by simulations of our model were consistent with the above mentioned characteristics of real data. We were also interested in identifying those aspects of the model that had the greatest influence on the qualitative behavior of the system.

Four separate sets of experiments were performed. The physiological accuracy of the model was enhanced with each successive set of experiments. In each case a neuronal system

[19]Distance over which response drops by a factor of e.

comprising of 1000 neurons with each neuron connected *randomly* to 100 other neurons was modeled.[20] The experiments were set up as follows.

Model:I 85% of all neurons in the system were randomly chosen to be excitatory (pyramidal) and the rest inhibitory (non-pyramidal). The response at the soma to a spike was modeled using the function $v(t) = \{\alpha Q/\sqrt{t}\}e^{-\beta/t}e^{-\gamma t}$ alluded to in section 2. The total response at the soma was computed as the sum of the responses to individual spikes. The strength of a synapse (Q) was chosen randomly from an uniform distribution over the range $[5.7, 15.7]$. Excitatory and inhibitory neurons were constructed to be physiologically identical in all respects save the strength of *inhibitory* synapses which were enhanced to six times the magnitude ($Q * 6.0$). The parameters α, β, and γ were set at fixed values for the entire system (same values as in figure 1). In other words, not only were all synapses assumed to be located at the same distance from the soma, but were also assumed to be generating identical (to a constant factor) responses. The synapses were assumed to have very short response times (≈ 10 $msec$) as is evident from figure 1. The lengths of the axonal collaterals and their variability were assumed to be uncharacteristically large, i.e., the time interval between the birth of a spike at a soma and its subsequent arrival across a synapse, indicating the length of the corresponding axonal collateral, was randomly chosen to lie between 5 $msec$ and 15 $msec$ (uniformly distributed). Refractoriness was modeled using a negative exponential function ($\mathcal{A}.e^{-\delta t}$) with $\mathcal{A}$ and δ held constant over the entire system.[21] The threshold was established in such a manner that at least 10 excitatory spikes (and no inhibitory spikes) with *coincident* peak impact[22] were required to cause a neuron to fire. The threshold was held constant over the entire system. The system was initialized with 5 live spikes per neuron chosen randomly over their respective lifetimes (≈ 200 spikes per second per neuron).

Model:II The lengths of the axonal collaterals as well as their variability were modified to reflect realistic dimensions; the time interval between the birth of a spike at a soma and its subsequent arrival across a synapse was randomly chosen to lie between 0.4 $msec$ and 0.9 $msec$. All other aspects of the model were left unchanged.

Model:III The restrictive assumption that all synapses be located at the same distance from the soma and in addition generate similar responses was eliminated. Instead, the locations of the synapses were chosen based on anatomical data. On the pyramidal cells, inhibitory synapses were cast randomly to within a distance of 0.3 space constants from the soma, and excitatory synapses were cast randomly from a distance of 0.3 to 3.0 space constants from the soma. On non-pyramidal cells both inhibitory and excitatory synapses were cast randomly between distances of 0.0 and 3.0 space constants from the soma. The more general function, $v(x,t) = \{\alpha Q/(x\sqrt{t})\}e^{-\beta x^2/t}e^{-\gamma t}$, was used to model the response to a spike at the soma. Since a synapse closer to the soma induced a more intense response, we were also able to eliminate the factitious assumption of inhibitory synapses being six times stronger than

[20] Simulating larger systems of neurons was found to be computationally intractable. Instead, we ran experiments on systems with 100 and 500 neurons. The qualitative characteristics of the dynamics that we shall describe later became more pronounced as the number of neurons in the system (and their degree of connectivity) was increased.

[21] Whereas in the abstract model, refractoriness must necessarily be continuously differentiable at $t = 0$, such restrictions do not apply here because the function is, in any case, discretized in time for simulation.

[22] The probability of 10 spikes arriving in such a manner that their peak impacts on a soma coincide is very low. The threshold was set such that on an average 20 spikes were required to cause a neuron to fire.

excitatory synapses. Next, 50% of all excitatory synapses were randomly chosen to be non-$NMDA$ synapses and the rest $NMDA$ synapses. Similarly, 50% of all inhibitory synapses were randomly chosen to be of type $GABA_A$ and the rest of type $GABA_B$. The characteristic response of each kind of synapse was modeled after graphs reported in (Bernander Douglas and Koch 1992) using the above potential function. Both the time and the shape of the response of respective kinds of synapses were modeled with reasonable fit. Finally, the threshold for firing of a neuron was reduced to an uncharacteristically low value and the system was initialized at a very sparsely active state ($\approx$ 20 spikes per second per neuron).
Model:IV The threshold for firing of a neuron was returned to its characteristic value, and the system was initialized at a more realistic state. (Two separate initializations, one with $\approx$ 100 spikes per second per neuron, and another with $\approx$ 150 spikes per second per neuron, were considered).

The dynamics of several random instantiations of each of the above models were investigated. In each case neurons were assigned a maximum number of effective spikes ($n = \lceil \Upsilon/r \rceil$) based on upper ($\Upsilon$) and lower ($r$) bounds computed from the above noted physiological parameters. Each system was initialized randomly and the ensuing dynamics was observed in the absence of all external inputs. Two classes of data were recorded. First, the temporal evolution of the total number of *active* spikes registered by the entire system was recorded as an approximation to EEG data, and second, individual spike trains of 10 randomly chosen neurons from each system were recorded for comparison with real spike train recordings.

4.3 Results

Figures 6, 7, 8, and 9 summarize the significant results from these simulations. Figure 6 displays normalized time series data pertaining to the total number of active spikes from representative instantiations of each model. Corresponding to each time series is also shown the results of a power spectrum analysis. When compared to real EEG recordings (Figure 7)[23] it becomes clear that the dynamical behavior of the model is qualitatively similar to that of the actual system. Moreover, the fact that the time series have spectra with broad bands rather than isolated peaks, and high noise level but nevertheless prominent structure, strongly suggests the possibility of chaos in these systems. Figure 8 displays 2-D phase portraits (scatter plots) of respective time series with the lag times (T) computed, as is conventional, as the earliest time that the auto-correlogram of a series crosses zero. Comparisons with analogous portraits derived from real EEG recordings (Babloyantz 1990) reinforce the claims of qualitative similarity.

Of the 10 neurons from each system whose spike trains were recorded during simulation, we chose one whose behavior we identified as representative of the mean. Figure 9 displays the time series of ISIs of these neurons (one per model), and their corresponding frequency distributions. The spike trains are not only aperiodic but their ISI distributions suggest that they could be generated from a poisson process.[24] We also computed the values of the coefficients of variation[25] for the various spike trains in order to partake in issues raised in

[23]The EEG data was down-loaded from http://www.scri.fsu.edu/~nayak/chaos/data.html. We thank Dr. Dennis Duke, and Dr. Krishna Nayak at SCRI, FSU for having consented to our use of the data.

[24]The distributions resemble the gamma density function $\Gamma(\lambda, 1)$.

[25]The ratio of the standard deviation to the mean of the ISI histogram ($\sigma_{\Delta t}/\overline{\Delta t}$).

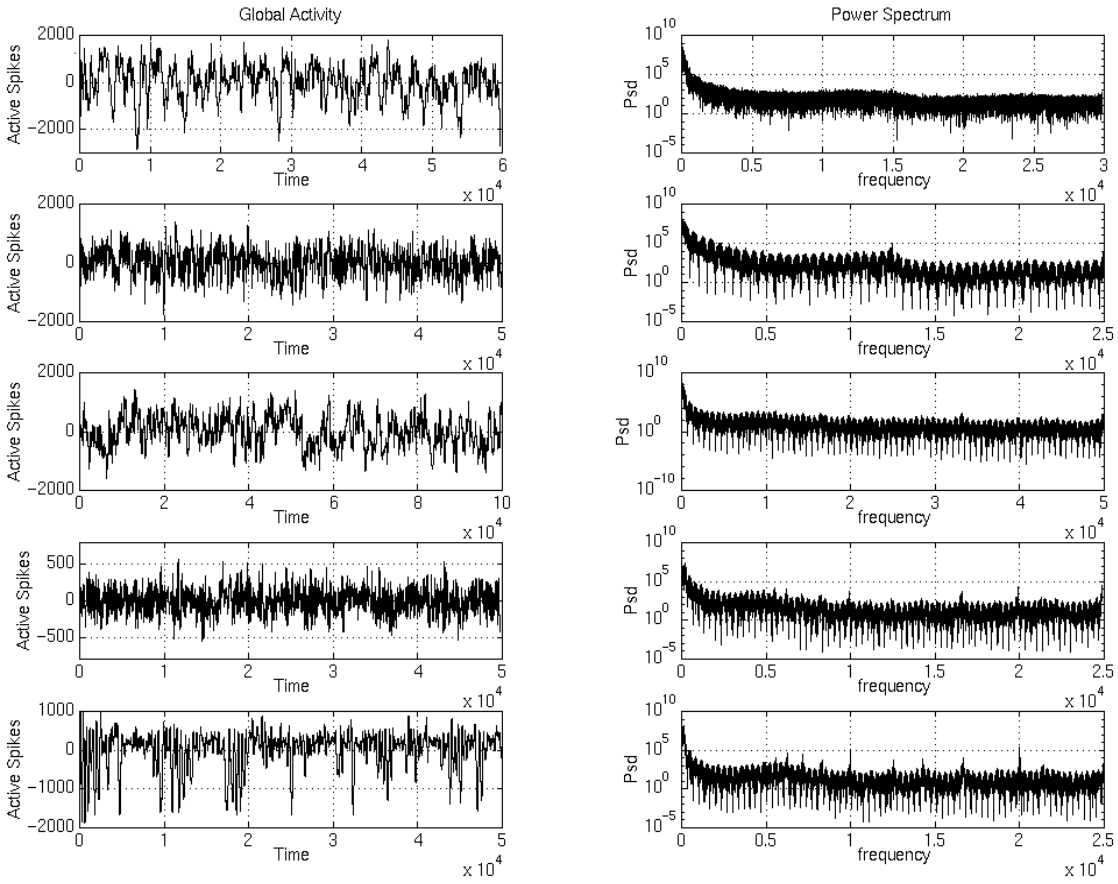

Figure 6: Normalized time series of total number of active spikes and corresponding Power Spectrums.

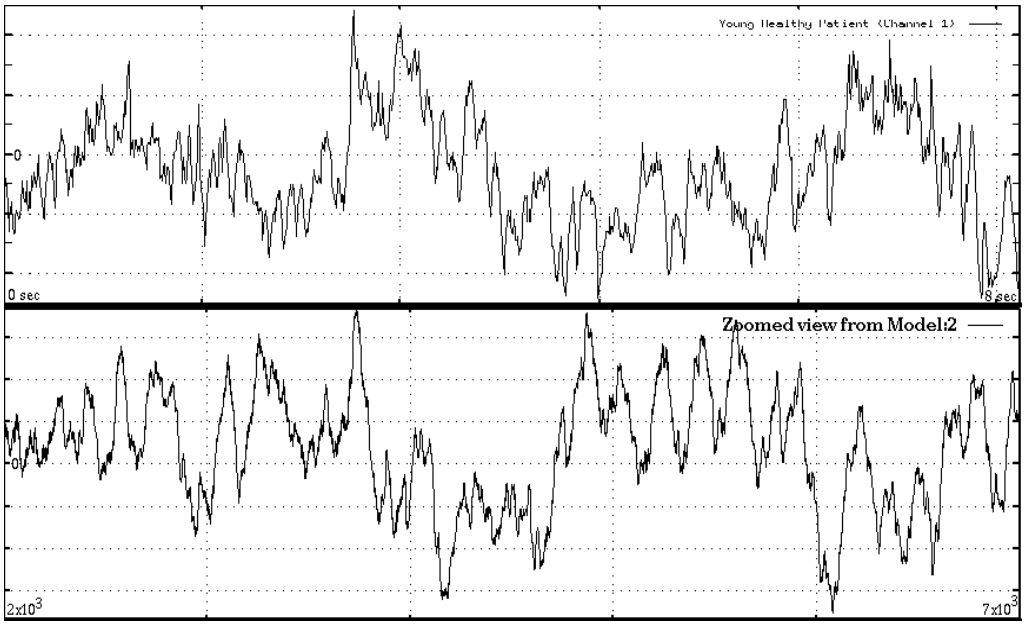

Figure 7: Top: Real EEG data from a healthy subject, and Bottom: Zoomed view of a section of data from Model:2 above.

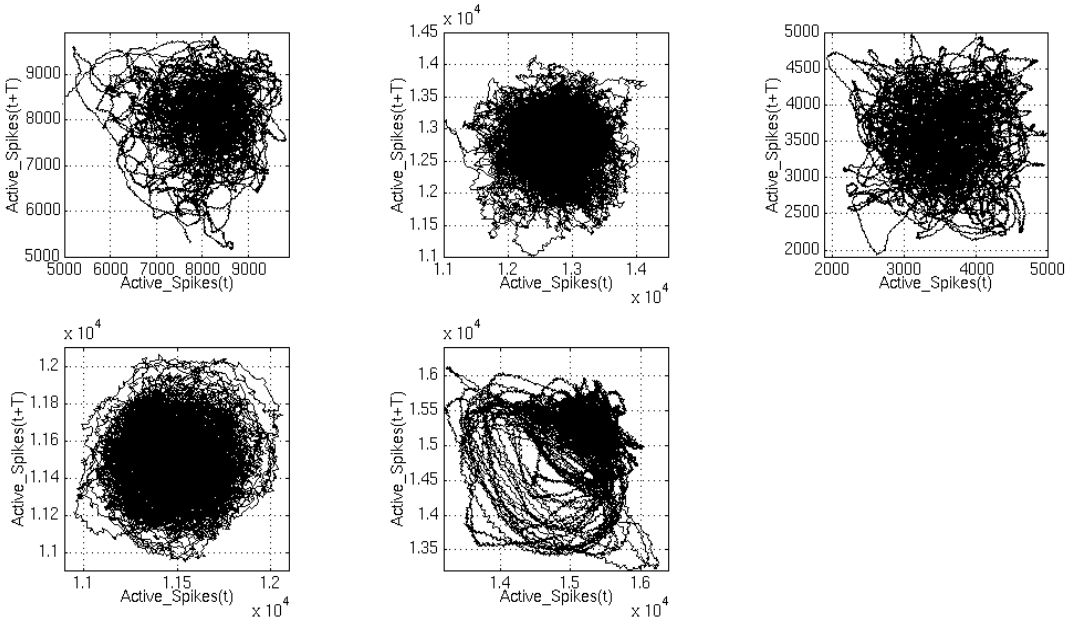

Figure 8: 2-D phase portraits derived from the above time series data.

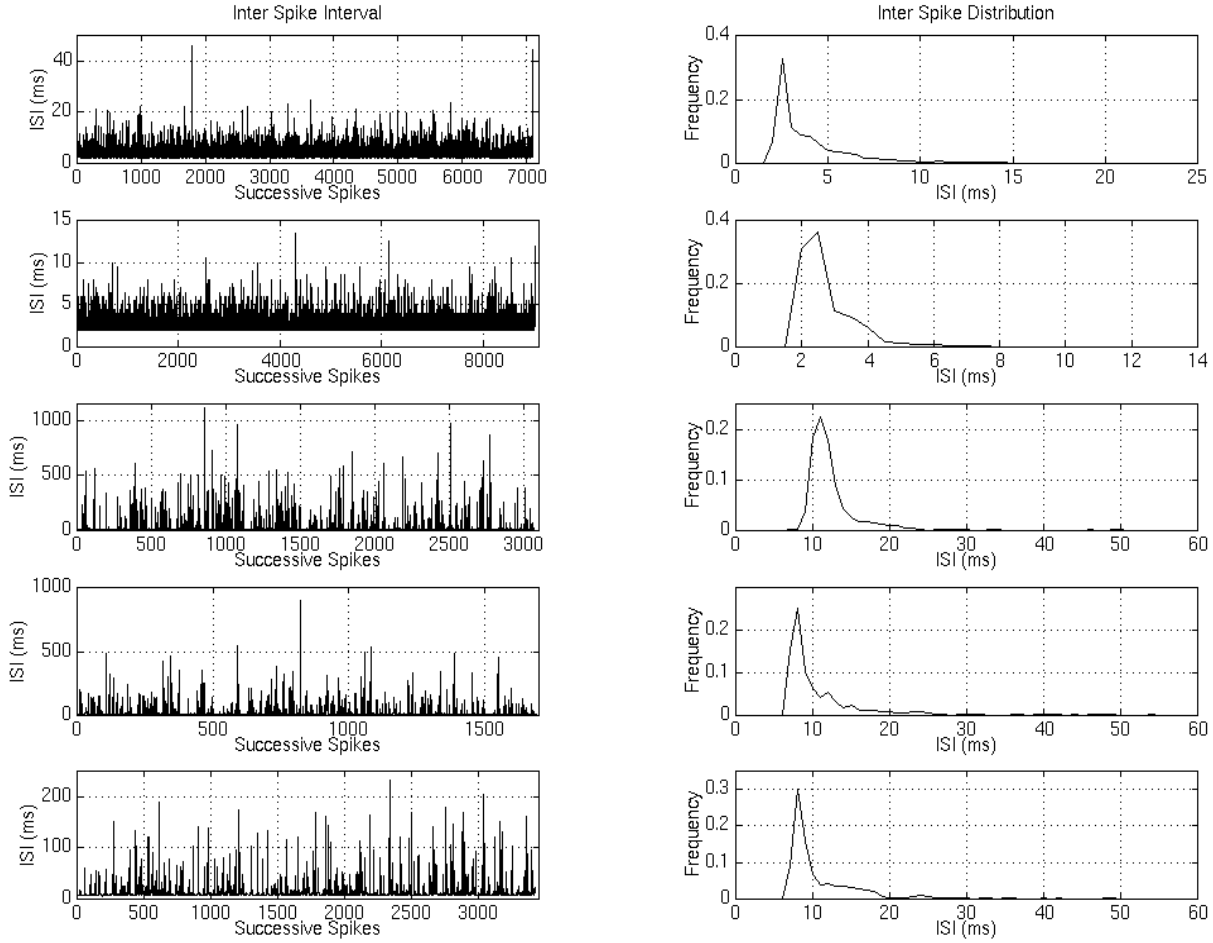

Figure 9: Inter Spike Interval recordings of representative neurons from each model and corresponding histograms.

(Softky and Koch 1992). The results obtained were encouraging; values ranged from 0.063 to 2.921 with the majority falling around 1.21.[26] Neurons with higher rates of firing tended to have lower values for the coefficient. The agreement between these values and real data speaks additionally in favor of the viability of our model. We now discuss various other outcomes from these experiments.

The above models, when viewed as concrete physical systems, come forth as substantially different from one another. The distinctions however, diminish considerably when they are regarded as specific realizations of one underlying abstract model. The issue then becomes how sensitive is the dynamics of the abstract model to the various parameters explored. One of the themes that emerged from the numerous experiments was that the qualitative behavior of the above models, from the simplest (Model:I) to the most realistic (Model:IV), was found to be strikingly similar. In other words, the outcome of the experiments unequivocally indicated that the *qualitative* dynamics of the model was stable with respect to variations in the afore mentioned parameters. It must be mentioned here that identical experiments were also conducted on systems consisting of 100 neurons with each neuron connected randomly to 10 other neurons. The resulting dynamics of these systems were found to be consistent with those of similar systems composed of 1000 neurons.

A second outcome from the experiments was the emergence of distinct patterns of aggregate behavior displayed by the systems of neurons. Three prominent classes of behavior were encountered. Each randomly generated instantiation of the model appeared to possess an intrinsic range of activity[27] over which the system was dynamically stable. If the system was initialized at an activity level below this range, the total number of active spikes dropped as the dynamics evolved, until the trivial fixed point of zero activity was reached. In contrast, if the system was initialized at an activity level above this range, the total number of active spikes rose until each neuron spiked *periodically* at a rate determined primarily by its absolute refractory period. In other words the system settled into a periodic cycle of intense regular activity resembling a state of seizure. When initialized within the range, the activity of the entire system waxed and waned *aperiodically* (see figure 6), while remaining at all times within the range.

The span of the above mentioned range was identified to be dependent on an assortment of parameters, most prominent among which were the proportion of inhibitory neurons in the system, their synaptic strengths, and their characteristic responses. Systems constructed from Models III and IV evinced larger intervals of stable activity. A closer inspection of the dynamics revealed the almost guardian-like role that the pool of inhibitory neurons played to the volatile tendencies of the excitatory neuron population. Two factors were found critical in the determination of the noted span. The first was the magnitude of the bounds (a) the maximum level of aggregate excitatory activity that the inhibitory pool, when fully operative, could subdue, and (b) the minimum level of aggregate excitatory activity that

[26](Softky and Koch 1992) report that the coefficients of variation for spike trains of fast-firing monkey visual cortex neurons lie between 0.5 and 1.1. Such high values, they claim, can not be accounted for by conventional stochastic biophysical models of the neuron. As the results clearly indicate, our deterministic model does accounts for this data.

[27]The claim is not that an exactly quantifiable region was identified in the state space; only that under conditions of relatively uniform activity a range with fuzzy boundaries was detected for the average spike frequency.

could recuperate once the inhibitory pool ceased to inhibit, and the second was the gradient of the characteristic response of the inhibitory neuron population in the neighborhood of these bounds, or in other words, the speed with which the inhibitory population responded to subdue increased activity as well as the speed with which it ceased when activity was sparse. These findings are in agreement with observations in (Erb and Aertsen 1992). It is our view that the afore mentioned range of stable activity is the range over which biological neuronal systems habitually operate, and is consequently of principal significance.

In all the experiments described above, the temporal evolution of the systems were considered in the *absence* of external inputs. The goal was to observe the innate behavioral characteristics of the systems. We conducted a second set of experiments to ascertain how predisposed the systems were to the above noted chaotic behavior in the presence of *regulating* external inputs. Each system was augmented with 2 pacemaker neurons, one excitatory and one inhibitory, that spiked at regular intervals.[28] The topology of the system was modified in a manner such that, of the 100 synapses on each neuron α received their inputs from one of the 2 pacemaker cells chosen randomly, and the remaining $(100 - \alpha)$ received their inputs from other neurons in the system. α was increased with successive experiments until the system was found to have settled into a periodic orbit. Figure 10 depicts the ISIs of 5 representative neurons each, from systems with α set at 70, 80, and 90. The discovery that the system did not quite settle into a periodic orbit even when 90% of all synapses were driven by periodic spikes bears witness to the system's propensity for chaotic behavior.

Finally, experiments were conducted to determine whether the systems were sensitive to initial conditions, a characteristic closely associated with chaotic behavior. Each system was initialized at two proximal points in state space and the resulting dynamics was recorded. Respective trajectories were either found to diverge strongly or become coincident.[29] Figure 11 depicts two trajectories that are just beginning to diverge. The individual phase space of a randomly chosen neuron is depicted in terms of an exhaustive array of two-dimensional projections.[30]

The reader will note that the results from the experiments reported in this section are substantially more qualitative than quantitative. The reason for this deliberate focus on qualitative aspects is as follows. The goal of the simulation experiments were not to emulate any *specific* neuronal mechanisms present in humans or in animals. Neither were the experiments intended to produce quantitative results about the model. The principal objective of the entire exercise was to demonstrate that the abstract model developed in the previous section was capable of modeling, adequately, the dynamics of local systems of neurons in the cerebral cortex. To this end, on the one hand values for the various parameters were chosen in such a manner that the resulting systems resembled *generic* cerebro-cortical neuronal systems, and on the other hand the dynamics of these systems were assessed only to the extent to which they conformed with the *generic* dynamics of cerebro-cortical neuronal systems. The experiments however generated more information than just the fact that the dynamics of the systems are indeed similar to that of the real systems. Through the numerous simulations also emerged various general dynamical characteristics of systems constructed from

[28] The two pacemaker cells spiked every $17th$ time step, generating the most basic periodic input.

[29] How this can happen is described in the next section.

[30] The graphs of a_0, a_{14},..., and a_8 are displayed in order.

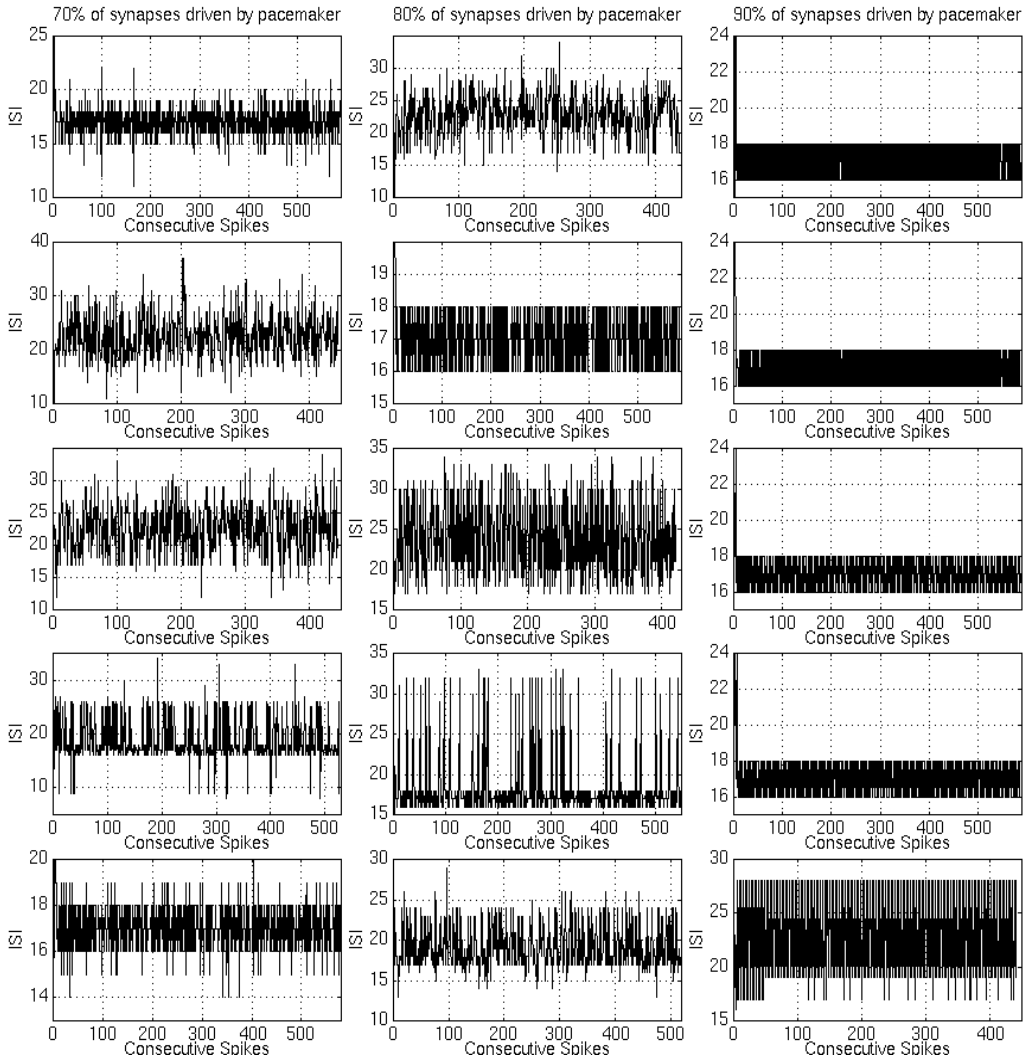

Figure 10: Inter Spike Interval recordings of representative neurons from systems driven by pacemaker cells. Three systems with 70%, 80%, and 90% of the synapses driven by two pacemaker cells are shown.

the abstract model. These characteristics provide an initial set of problems for consideration during the formal analysis of the model.

Finally, the results of the experiments also shed light on why the strictly neurophysiological perspective to the study of the brain faces profound problems, and why results have been so difficult to come by in the field. Whereas the abstract model defined in the previous section contains a good deal of structure, such is not easily revealed in its dynamics. This is more so in the case of real neurophysiological data wherein the impression is one of an appalling lack of structure. The incongruence between data recorded at the individual or local neuronal level and at the behavioral level is enormous. Bridging this gap without access to an intermediary model is a formidable task. Whereas approaching the problem via a model might be deemed weaker because acceptance of the results hinge upon the acceptance of the adequacy of the model, it is our view that given the circumstances, this is arguably the only

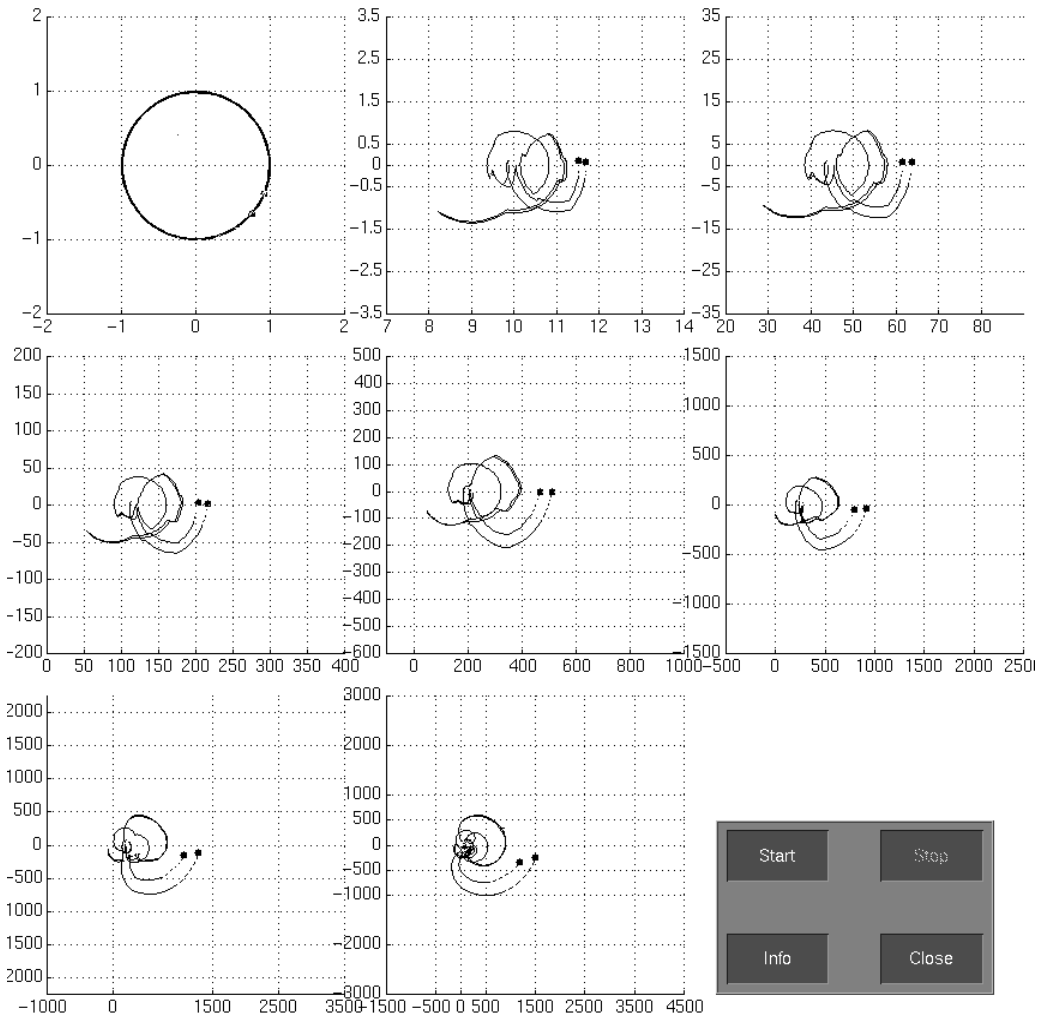

Figure 11: Two trajectories that are just beginning to diverge. The 2-D projections a_0, a_{14}, ..., and a_8 of the phase space of a single neuron are shown in order of left to right, and top to bottom.

viable approach.

Appendix: I

Proof of Theorem 1:
The proof of Theorem 1 is based on the following two theorems (4 and 5).

Theorem 4 *Necessary and sufficient conditions for all roots of* $f(z) = z^n + a_{n-1}z^{n-1} + ... + a_0$ *to be* distinct *and to lie on the unit circle,* $|z| = 1$, *are*
(a) $|a_0| = 1$, *and* $a_i = \bar{a}_{n-i}.a_0$, *for* $i = 1, 2, ..., n-1$. *and*
(b) $f'(z)$ *has all its roots* strictly *inside* $|z| = 1$.
Proof:

(i) Distinct roots on $|z| = 1$ implies (a) and (b) above.

We have assumed w.l.o.g that $a_n = 1$. We are given $f(z) = a_n z^n + a_{n-1} z^{n-1} + ... + a_0 = a_n \prod_{j=1}^{n} (z - z_j)$, and furthermore, $f^*(z)$ defined as $z^n \bar{f}(1/z) = \bar{a}_0 z^n + \bar{a}_1 z^{n-1} + ... + \bar{a}_n = \bar{a}_0 \prod_{j=1}^{n} (z - z_j^*)$. It is clear from the definition of $f^*(z)$ that its roots lie at $z_i^* = (1/\bar{z}_i)$. Since $\forall i, |z_i| = 1$ implies $\forall i, (1/\bar{z}_i) = z_i$, the roots of $f(z)$ and $f^*(z)$ are identical. Therefore, $\bar{a}_0/a_n = \bar{a}_1/a_{n-1} = ... = \bar{a}_n/a_0$. Introducing $a_n = 1$ we get $|a_0| = 1$, and $a_i = \bar{a}_{n-i}.a_0$, for $i = 1, 2, ..., n-1$. as a set of necessary *criteria.*

The proof of the assertion that all roots of $f'(z)$ lie strictly within the unit circle, $|z| = 1$, is based on Lucas Theorem *which states that any convex polygon that contains all the roots of a complex polynomial $f(z)$ also contains all the roots of its derivative $f'(z)$. Obviously then, no root of $f'(z)$ lies outside $|z| = 1$. Moreover, for a root of $f'(z)$ to lie on $|z| = 1$, $f(z)$ must have a root at the same location which makes it a multiple root of $f(z)$ contradicting the assumption that the roots of $f(z)$ are distinct. All roots of $f'(z)$ therefore lie strictly inside $|z| = 1$.*

(ii) (a) and (b) above imply distinct roots on $|z| = 1$.

We note that (b) above enforces that $f(z)$ can not have multiple roots, for if it did, $f'(z)$ would have a root on $|z| = 1$, contradicting (b). Therefore, it only needs to be shown that the roots of $f(z)$ lie on $|z| = 1$.

Lemma 1 (Cohn) *If the coefficients of the polynomial $g(z) = b_m z^m + b_{m-1} z^{m-1} + ... + b_0$ satisfy the relations,*
$b_m = u\bar{b}_0, \quad b_{m-1} = u\bar{b}_1, ..., b_0 = u\bar{b}_m,$
then $g(z)$ has in the circle $|z| < 1$ as many roots as the polynomial
$g_1(z) = [g'(z)]^* = z^{m-1} \bar{g}'(1/z) = \sum_{j=0}^{m-1} b_j^{(1)} z^j$.
where $g'(z)$ is the derivative of $g(z)$.

$f(z)$ by criterion (a) satisfies $a_n = u\bar{a}_0, \quad a_{n-1} = u\bar{a}_1, ..., a_0 = u\bar{a}_n$ with $u = a_0$.
Therefore, based on the above lemma, $f(z)$ has in circle $|z| < 1$ as many roots as $[f'(z)]^*$. Since (b) enforces that all the roots of $f'(z)$ are strictly inside $|z| < 1$, $[f'(z)]^*$ has no roots inside $|z| < 1$. (By definition, any root z_i^* of $[f'(z)]^*$ is given by $z_i^* = 1/\bar{z}_i$.) So f(z) has no roots inside $|z| < 1$. Finally, the condition $|a_0| = 1$ constraints all roots of $f(z)$ to lie on $|z| = 1$.

QED.

Theorem 5 *The set of criteria, $\delta_1 < 0$ and $\delta_j > 0 \quad$ for $j = 2, 3, ..., n-1$. as described in Theorem 1 is* **equivalent** *to the criterion that all roots of $f'(z)$ lie strictly inside the unit circle, $|z| = 1$.*

Proof:

(i) The criteria implies all roots of $f'(z)$ lie strictly inside $|z| = 1$.

Follows directly from the following theorem by Marden.

Lemma 2 (Marden) *If for polynomial* $f(z) = a_n z^n + a_{n-1} z^{n-1} + ... + a_0$ *the sequence* $\langle f_0(z), f_1(z), ..., f_n(z) \rangle$ *is constructed as* $f_j(z) = \sum_{k=0}^{n-j} a_k^{(j)} z^k$ *where* $f_0(z) = f(z)$ *and* $f_{j+1}(z) = \bar{a}_0^{(j)} f_j(z) - a_{n-j}^{(j)} f_j^*(z), \quad j = 0, 1, ..., n-1$ *and* $\delta_{j+1} = a_0^{(j+1)}$ *satisfy the criteria,* $\delta_1 < 0$ *and* $\delta_2, ..., \delta_n > 0$ *then f(z) has all n roots strictly inside the unit circle* $|z| = 1$.

(ii) All roots of $f'(z)$ *lie strictly inside* $|z| = 1$ *implies the criteria.*

(a) We first show that $\delta_1 < 0$.
Since $f'(z) = f_0(z) = b_{n-1} z^{n-1} + ... + b_1 z + b_0$ *has all roots strictly inside* $|z| = 1$, *the modulus of the product of all roots is strictly less than 1, i.e.,* $|b_0/b_n| < 1$. *So* $|b_0| < |b_n|$, *and* $\delta_1 = |b_0|^2 - |b_n|^2 < 0$.
(b) The proof for $\delta_2, \delta_3, ..., \delta_n > 0$ *is based on the following theorem by Marden.*

Lemma 3 (Marden) *If in Lemma 2,* $f_j(z)$ *has* p_j *roots in the unit circle and no roots on it and if* $\delta_{j+1} \neq 0$ *then* $f_{j+1}(z)$ *has* $p_{j+1} = \frac{1}{2}\{n - j - [(n-j) - 2p_j] sgn\delta_{j+1}\}$ *roots in the unit circle and none on it.*

We have assumed $f_0(z) = f'(z)$ *has all* $n-1$ *roots in the unit circle and none on it. We have also shown that* $\delta_1 \neq 0$, *in fact,* $\delta_1 < 0$. *Therefore,* $sgn\delta_1 = -1$. *Based on the above lemma then,* $f_1(z)$ *has* $p_1 = 0$ *roots in the unit circle and none on it. In other words, all the roots of* $f_1(z)$ *lie outside the unit circle. Using the argument in (a) above we get,* $\delta_2 > 0$. *We now apply the lemma repeatedly to get* $p_2 = \frac{1}{2} p_1 = 0$ *and so on, implying that* $\delta_3, ..., \delta_n > 0$.
QED.

Proof of Theorem 2:
The proof for Theorem 2 is based on the following theorem. $\overline{\mathbb{L}_n}$ below denotes the closure of $\mathbb{L}_n$ in the corresponding space.

Theorem 6 *If* $x \in \overline{\mathbb{L}_n}$, *and* $x \notin \mathbb{L}_n$ *then* x *denotes a polynomial with all roots on* $|z| = 1$ *and at least one multiple root. Conversely, if a polynomial has all roots on* $|z| = 1$ *and at least one multiple root then the corresponding point* x *in the transformed space satisfies* $x \in \overline{\mathbb{L}_n}$ *and* $x \notin \mathbb{L}_n$.
Proof:
(i) $x \in \overline{\mathbb{L}_n}$, $x \notin \mathbb{L}_n$ *implies multiple roots.*

Since x *is a limit point of* $\mathbb{L}_n$, $\exists$ *a denumerable sequence of points,* $\langle y_1, y_2, ..., y_k, y_{k+1}, ... \rangle$ *in* $\mathbb{C}^{\lfloor n/2 \rfloor} \times S^1$ *(*$\mathbb{C}^{\lfloor n/2 \rfloor - 1} \times \mathbb{M}^2$*) such that* $\forall i \; y_i \in \mathbb{L}_n$ *and* $\lim_{n \to \infty} y_i = x$. *We now apply the following theorem by Coolidge to this sequence.*

Lemma 4 (Coolidge) *Given two algebraic equations of the same degree, so related that the coefficients of the first are constant, and that of the highest power of the variable is not zero, while those of the second approach the corresponding coefficients of the first as limits, then the roots of the two equations, where each multiple root of order* k *is counted* k *times as* k *roots, may be put into such a one-to-one correspondence that the absolute value of the difference between each two corresponding roots approach zero.*

Since $x \notin \mathbb{L}_n$, either the polynomial does not have all roots on $|z| = 1$, or not all roots are distinct, or both. If the polynomial does not have all roots on the unit circle, the distance between at least one set of roots in the above theorem is bounded from below thus contradicting it.

(ii) Multiple roots imply $x \in \overline{\mathbb{L}}_n$, $x \notin \mathbb{L}_n$.

Since the roots of the polynomial corresponding to x are not all distinct, $x \notin \mathbb{L}_n$. We construct a denumerable sequence of sets of roots such that each set comprises of distinct roots on $|z| = 1$ and there is a many-to-one correspondence between positions in the sets and the roots of the given polynomial such that roots in each such position converge to the corresponding root of x.

Let $\langle z_1, z_2, ..., z_n \rangle$ be the roots of the polynomial corresponding to x with multiple roots of order k repeated k times. Let $\delta > 0$ be chosen such that $\delta < |(1/2) min_{\forall i,j \ z_i \neq z_j}(\angle(z_i/z_j))|$. Let $\langle \delta_1, \delta_2, ..., \delta_n \rangle$ be chosen such that $\forall i, j \ s.t. \ i \neq j, \ \delta_i \neq \delta_j$ and $\forall i, \ 0 < |\delta_i| < \delta$.

We consider the sequence of sets $\langle z_1.e^{i(\delta_1/2^p)}, z_2.e^{i(\delta_2/2^p)}, ..., z_n.e^{i(\delta_n/2^p)} \rangle$ for p=0,1,... and note that it satisfies the stated criteria and converges absolutely to $\langle z_1, z_2, ..., z_n \rangle$. Since each coefficient is a continuous function of all roots, the sequence of polynomials $\langle y_1, y_2, ..., y_k, y_{k+1}, ... \rangle$ corresponding to the sets of roots in the above sequence satisfy $\forall i \ y_i \in \mathbb{L}_n$ and $\lim_{n\to\infty} y_i = x$. x is therefore a limit point of $\mathbb{L}_n$.

QED.

Appendix: II

Let $F^{-1} : \overline{\mathbb{L}}_n \to \mathbb{U} \subset \mathbb{R}^n$ denote the function that maps the transformed space of an individual neuron into its initial space ($F^{-1}\langle a_{n-1}, ..., a_{\lceil n/2 \rceil}; \angle a_0 \rangle = \langle x^1, ..., x^n \rangle$ for odd n, and $F^{-1}\langle a_{n-1}, ..., |a_{\lceil n/2 \rceil}|; \angle a_0 \rangle = \langle x^1, ..., x^n \rangle$ for even n, such that $0 \leq x^1 \leq x^2 \leq ... \leq x^n \leq 2\pi$). Let $G(.)$ denote the Cartesian product of $F^{-1}(.)$ with itself appropriately many times that maps the transformed space of all relevant neurons into their initial spaces. We define $\widetilde{P} = P \circ G$, and note immediately that it is a continuous function. Moreover, since

$$\frac{\partial \widetilde{P}}{\partial a_i} = \sum_j \frac{\partial P}{\partial x^j} \frac{\partial x^j}{\partial a_i}$$

$\widetilde{P}(.)$ is C^1 at all locations where $\frac{\partial x^j}{\partial a_i}$ is well defined for all i and j.

Theorem 7 *$\frac{\partial x^j}{\partial a_i}$ is undefined when x^j is a multiple root, i.e., if $\exists a, b \ s.t. \ x^a = x^b$, then $Det(DF) = 0$.*

Proof:

We note that $\forall j \ a_j$ is a symmetric function of $(x^1, ..., x^n)$. Therefore, $\forall j \ \frac{\partial a_j}{\partial x^a} = \frac{\partial a_j}{\partial x^b}$ when $x^a = x^b$. In other words, if $x^a = x^b$, columns "a" and "b" in (DF) are identical.

QED.

Theorem 8 *If $\forall i, j \ (i \neq j \Rightarrow x^i \neq x^j)$, then $Det(DF) \neq 0$.*

Proof:

We prove the theorem for cases, n is odd and n is even, separately.

(i) n is odd.

In this case,

$$DF = \begin{pmatrix} \frac{\partial \angle a_0}{\partial x_1} & \frac{\partial \angle a_0}{\partial x_2} & \cdots & \frac{\partial \angle a_0}{\partial x_n} \\ \frac{\partial \Re a_{\lceil n/2 \rceil}}{\partial x_1} & \frac{\partial \Re a_{\lceil n/2 \rceil}}{\partial x_2} & \cdots & \frac{\partial \Re a_{\lceil n/2 \rceil}}{\partial x_n} \\ \frac{\partial \Im a_{\lceil n/2 \rceil}}{\partial x_1} & \frac{\partial \Im a_{\lceil n/2 \rceil}}{\partial x_2} & \cdots & \frac{\partial \Im a_{\lceil n/2 \rceil}}{\partial x_n} \\ \vdots & \vdots & \ddots & \vdots \\ \frac{\partial \Re a_{n-1}}{\partial x_1} & \frac{\partial \Re a_{n-1}}{\partial x_2} & \cdots & \frac{\partial \Re a_{n-1}}{\partial x_n} \\ \frac{\partial \Im a_{n-1}}{\partial x_1} & \frac{\partial \Im a_{n-1}}{\partial x_2} & \cdots & \frac{\partial \Im a_{n-1}}{\partial x_n} \end{pmatrix}$$

Computing the value for (DF) at $\langle z_1, z_2, ..., z_n \rangle = \langle e^{i\theta_1}, e^{i\theta_2}, ..., e^{i\theta_n} \rangle$ *based on,*

a) $\forall j,\ \frac{\partial \angle a_0}{\partial x_j}|_{\langle z_1, z_2, ..., z_n \rangle} = 1.$

b) $\forall j,\ \frac{\partial \Re a_{n-1}}{\partial x_j}|_{\langle z_1, z_2, ..., z_n \rangle} = \frac{i}{2}[z_j - \bar{z}_j].$

c) $\forall j,\ \frac{\partial \Im a_{n-1}}{\partial x_j}|_{\langle z_1, z_2, ..., z_n \rangle} = \frac{1}{2}[z_j + \bar{z}_j].$

d) $\forall j,\ \frac{\partial \Re a_{n-2}}{\partial x_j}|_{\langle z_1, z_2, ..., z_n \rangle} = \frac{i}{2}[z_j \sum_{i \neq j} z_i - \bar{z}_j \sum_{i \neq j} \bar{z}_i].$

e) $\forall j,\ \frac{\partial \Im a_{n-2}}{\partial x_j}|_{\langle z_1, z_2, ..., z_n \rangle} = \frac{1}{2}[z_j \sum_{i \neq j} z_i + \bar{z}_j \sum_{i \neq j} \bar{z}_i]$. *and so forth,*

and algebraically manipulating the rows of (DF), we get

$$DF = \begin{pmatrix} 1 & 1 & \cdots & 1 \\ \sin(\theta_1) & \sin(\theta_2) & \cdots & \sin(\theta_n) \\ \cos(\theta_1) & \cos(\theta_2) & \cdots & \cos(\theta_n) \\ \sin(2\theta_1) & \sin(2\theta_2) & \cdots & \sin(2\theta_n) \\ \cos(2\theta_1) & \cos(2\theta_2) & \cdots & \cos(2\theta_n) \\ \vdots & \vdots & \ddots & \vdots \\ \sin(\frac{n-1}{2}\theta_1) & \sin(\frac{n-1}{2}\theta_2) & \cdots & \sin(\frac{n-1}{2}\theta_n) \\ \cos(\frac{n-1}{2}\theta_1) & \cos(\frac{n-1}{2}\theta_2) & \cdots & \cos(\frac{n-1}{2}\theta_n) \end{pmatrix}$$

We now prove $Det(DF) \neq 0$ *by demonstrating that the only vector* $\vec{x}$ *that satisfies* $\vec{x}(DF) = 0$ *is the zero vector.*

We set $n = 2m + 1$, *and consider the function* $f(x) = \alpha_0 + \alpha_1 \sin x + \alpha_2 \cos x + ... + \alpha_{2m-1} \sin mx + \alpha_{2m} \cos mx$. *For arbitrary reals* $\alpha_0, \alpha_1, ...\alpha_{2m}$ *not all zero, we demonstrate that the* maximum *number of roots that* $f(x)$ *can have in* $[0, 2\pi)$ *is* 2m, *thus proving the above claim.*

For arbitrary reals $\alpha_0, \alpha_1, ...\alpha_{2m}$ *not all zero, we can construct the function* $g(x) = \gamma_0 + \gamma_1 \sin(x + \beta_1) + \gamma_2 \sin(2x + \beta_2) + ... + \gamma_m \sin(mx + \beta_m)$ *such that* $g(x) \equiv f(x)$, *and reals* $\gamma_0, \gamma_1, \beta_1, ..., \gamma_m, \beta_m$ *are not all zero. Since* $g(x)$ *is a periodic function with period* 2π, *if* $g(x)$ *has* μ *roots in* $[0, 2\pi)$ *then* $g^1(x) = g'(x)$ *has* at least μ *roots in* $[0, 2\pi)$ *and since* $g^1(x)$ *is also periodic with period* 2π, $g^2(x) = g''(x)$ *has* at least μ *roots in* $[0, 2\pi)$ *and so on. Since*

$$g^{4k}(x) = \gamma_1 \sin(x + \beta_1) + 2^{4k}\gamma_2 \sin(2x + \beta_2) + ... + m^{4k}\gamma_m \sin(mx + \beta_m) \text{ for } k = 1, 2, 3, ...$$

(a) The coefficients of $\sin(x + \beta_1), \sin(2x + \beta_2), ...,$ *and* $\sin((m-1)x + \beta_{m-1})$ *can be made negligibly small as compared to the coefficient of* $\sin(mx + \beta_m)$ *by increasing* k, *and*

(b) If the leading term, $m^{4k}\gamma_m \sin(mx+\beta_m)$, is disregarded, the residual can be approximated by $(m-1)^{4k}\gamma_{m-1}\sin((m-1)x+\beta_{m-1})$; a function that oscillates at a frequency lower than that of the leading term.
Based on these considerations and the fact that $m^{4k}\gamma_m \sin(mx+\beta_m)$ has 2m roots in $[0,2\pi)$, we conclude that $\mu \leq 2m$.

(ii) n is even.

In (i) above we showed that if n=2m+1 and $\forall i,j(i \neq j \Rightarrow \theta_i \neq \theta_j)$ then $F : \mathbb{U} \rightarrow \overline{\mathbb{L}}_n$, $F\langle x^1,...,x^n\rangle = \langle a_{n-1},...,a_{\lceil n/2\rceil};\angle a_0\rangle$ is a C^1 diffeomorphism *in an open set around $\langle\theta_1,\theta_2,...,\theta_n\rangle$, and therefore so is F^{-1}.*

We now set n=2m and note that given arbitrary θ^*, $F\langle x^1,...x^{2m}\rangle = \langle a_{n-1},...,|a_{\lceil n/2\rceil}|;\angle a_0\rangle$ is a C^1 diffeomorphism in an open set around $\langle\theta_1,\theta_2,...,\theta_{2m}\rangle$ if and only if function F' which is identical to F except for an additional variable that maps to itself, $F'\langle x^1,...,x^{2m};x^{2m+1}\rangle = \langle a_{n-1},...,|a_{\lceil n/2\rceil}|;\angle a_0;x^{2m+1}\rangle$ is a C^1 diffeomorphism in an open set around $\langle\theta_1,\theta_2,..,\theta_{2m},\theta^*\rangle$.

Consequently, all that needs to be shown is that for n=2m, the mapping $\langle a_{2m-1},...,|a_m|;\angle a_0;x^{2m+1}\rangle \rightarrow \langle A_{2m},...,A_{m+1};\angle A_0\rangle$ is C^1 (A_i's represent the coefficients of the complex polynomial of degree 2m+1 whose roots include the additional $e^{i\theta^*}$). Based on (i) above we will then have proved the theorem for even n. Note that the constraints $\forall i,j\ (i \neq j \Rightarrow \theta_i \neq \theta_j)$ and $\forall i = 1...2m\ \theta_i \neq \theta^*$ are enforced by (i) on the mapping $\langle A_{2m},...,A_{m+1};\angle A_0\rangle \rightarrow \langle x^1,...,x^{2m};x^{2m+1}\rangle$.

Comparing coefficients of corresponding terms, we get

$$
\begin{aligned}
&A_{2m} = a_{2m-1} - e^{ix^{2m+1}}\\
&A_{2m-1} = a_{2m-2} - a_{2m-1}e^{ix^{2m+1}}\\
&\vdots\\
&A_{m+1} = |a_m|e^{\frac{i}{2}\angle a_0} - a_{m+1}e^{ix^{2m+1}} \text{ and}\\
&A_0 = a_0 e^{ix^{2m+1}}
\end{aligned}
$$

which immediately demonstrates that the mapping is C^1.

QED.

Even though we defined the phase space of a neuron to be $\overline{\mathbb{L}}_n$, the portion of it that is actually explored by the state dynamics of the neuron has multiple roots ($x^i = x^j$) only when $x^i = x^j = 0 = 2\pi$, i.e., when the spikes are dead and are stationed in the abstract buffer.

In view of this, we define $\widetilde{P}$ as follows:

- If roots $\langle z_1,z_2,...,z_n\rangle \equiv \langle e^{ix^1},e^{ix^2},...,e^{ix^n}\rangle$ are all distinct then $\frac{\partial\widetilde{P}}{\partial a_i} = \sum_j \frac{\partial P}{\partial x^j}\frac{\partial x^j}{\partial a_i}$, where $\frac{\partial x^j}{\partial a_i}$ are the elements of $(DF)^{-1}$.
- If roots $\langle e^{ix^1},e^{ix^2},...,e^{ix^n}\rangle$ are not all distinct, and e^{ix^k} is one such multiple root (occurring at e^{i0}), then we *define* $\forall k$ such that k is a multiple root, $\frac{\partial P}{\partial x^k}\frac{\partial x^k}{\partial a_i} = 0$. Even though $\frac{\partial x^k}{\partial a_i}$ is undefined in such a case, based on the assumption that $\frac{\partial P}{\partial x^k} = 0$ over an

infinitesimal interval, ($e^{i\delta} > e^{ix^k} > e^{i(2\pi-\delta)}$), we can maintain continuous differentiability of $\widetilde{P}$. Note however, that in doing so we have imposed an additional constraint on $P(.)$, and consequently on $P_{Afferent}(.)$ and $P_{Refractory}(.)$. Informally stated, this requires that for an infinitesimal interval before the death of a spike and the same after the inception of a spike, its effect on the cross-membrane potential of any neuron is zero. The previously stated criteria for the inception of a spike, namely, $P(.) = T$ and $dP(.)/dt \geq 0$ complements this constraint and maintains consistency in the model.

- If roots $\langle e^{ix^1}, e^{ix^2}, ..., e^{ix^n}\rangle$ are not all distinct, but e^{ix^k} is a distinct root, $\frac{\partial x^k}{\partial a_i}$ can not be directly computed from $(DF)^{-1}$ since $det(DF) = 0$. However, as is shown next, it can be extracted indirectly.

Theorem 9 *Let the roots of the polynomial $f(z) = z^n + a_{n-1}z^{n-1} + ... + a_0$, constrained to have all roots on the unit circle, be $\langle e^{ix^1}, e^{ix^2}, ..., e^{ix^n}\rangle$. Let $e^{ix^i} = e^{ix^j}$ and all other roots be distinct. Let the sequence $\{\langle y_1^1, y_1^2, ..., y_1^n\rangle\langle y_2^1, y_2^2, ..., y_2^n\rangle\langle ...\rangle ...\}$ be constructed such that $\forall i, j\ y_i^j$ is distinct and $\forall j\ lim_{i\to\infty} y_i^j = x^j$. Then $\forall i\ (DF)^{-1}|_{\langle e^{iy_i^1}, e^{iy_i^2}, ..., e^{iy_i^n}\rangle}$ is well defined and limiting values exist for $\frac{\partial x^k}{\partial a_l}$ for all $k \neq i$ or j.*

Proof:

That $\forall i\ (DF)^{-1}|_{\langle e^{iy_i^1}, e^{iy_i^2}, ..., e^{iy_i^n}\rangle}$ is well defined is obvious from the previous theorem and that $\forall i, j\ y_i^j$ is distinct. However, at $\langle e^{ix^1}, e^{ix^2}, ..., e^{ix^n}\rangle$ we have shown that columns "i" and "j" in (DF) become identical. We now refer to the simplified version of (DF) computed at $\langle e^{i\theta_1}, e^{i\theta_2}, ..., e^{i\theta_n}\rangle$ in the previous theorem.

In the limiting case, column "j" can be replaced by [column "i"+($\frac{d}{d\theta}$ column "i")$\times\Delta\theta$], where $\Delta\theta \to 0$. Subtracting column "i" and extracting $\Delta\theta$ as a non-zero constant, one gets, column "j" $\equiv \langle 0, \cos(\theta_i), -\sin(\theta_i), 2\cos(2\theta_i), -2\sin(2\theta_i), ...\rangle^T$.

It is easily demonstrated that this modified matrix is invertible based on the same technique as employed in the previous theorem. Once again we consider the function $g(x) = \gamma_0 + \gamma_1 \sin(x + \beta_1) + \gamma_2 \sin(2x + \beta_2) + ... + \gamma_m \sin(mx + \beta_m)$ and ask for arbitrary reals $\gamma_0, \gamma_1, \beta_1, ..., \gamma_m, \beta_m$ not all zero, whether $g(x)$ can have 2m distinct roots and 1 multiple root in $[0, 2\pi)$. The answer, as in the previous case, is no *because $g^1(x)$ must have at least 2m+1 roots and so on.*

All rows except "i" and "j" in $(DF)^{-1}$ (computed as $(DF)^{-1}(DF) = I$), therefore have finite limiting values.

QED.

Appendix: III

Proof of Theorem 3:
If $b_{n-k} = a_{n-k}/(-1)^k$, then $b_{n-k} = \sum_{i_1\neq i_2\neq ...\neq i_k} z_{i_1} z_{i_2} ... z_{i_k}$. We prove that $db_0/dt = (2\pi i/\Upsilon)(n - \sigma)b_0$, and $db_{n-k}/dt = (2\pi i/\Upsilon)[k(b_{n-k} - {}^{\sigma}C_k) - \sigma\sum_{j=1}^{k-1}(-1)^{k-1-j}(b_{n-j} - {}^{\sigma}C_j)]$ and the theorem follows.

We begin with the set of roots not at e^{i0}, i.e., $\langle z_1, z_2, ..., z_\sigma\rangle$ and note immediately that $b_{n-k} = {}^{\sigma}C_k + {}^{\sigma}C_{k-1}\sum_{i_1} z_{i_1} + {}^{\sigma}C_{k-2}\sum_{i_1\neq i_2} z_{i_1} z_{i_2} + ... + {}^{\sigma}C_0 \sum_{i_1\neq i_2\neq ...\neq i_k} z_{i_1} z_{i_2} ... z_{i_k}$. (All stationary roots are set at $e^{i0} = 1$.)

It follows that
$db_{n-k}/dt = (2\pi i/\Upsilon)[1.{}^{\sigma}C_{k-1} \sum_{i_1} z_{i_1} + 2.{}^{\sigma}C_{k-2} \sum_{i_1 \neq i_2} z_{i_1} z_{i_2} + ... +$
$(k-1).{}^{\sigma}C_1 \sum_{i_1 \neq i_2 \neq ... \neq i_{k-1}} z_{i_1} z_{i_2} ... z_{i_{k-1}}] + d/dt \sum_{i_1 \neq i_2 \neq ... \neq i_k} z_{i_1} z_{i_2} ... z_{i_k}$.
Or equivalently,
$db_{n-k}/dt = (2\pi i/\Upsilon)[k(b_{n-k} - {}^{\sigma}C_k) -$
$\{(k-1).{}^{\sigma}C_{k-1} \sum_{i_1} z_{i_1} + (k-2).{}^{\sigma}C_{k-2} \sum_{i_1 \neq i_2} z_{i_1} z_{i_2} + ... + 1.{}^{\sigma}C_1 \sum_{i_1 \neq i_2 \neq ... \neq i_{k-1}} z_{i_1} z_{i_2} ... z_{i_{k-1}}\}]$.

We now prove by induction that
$\sigma \sum_{i=n}^{0} (-1)^{n-i}.\ {}^{\sigma}C_i = (n+1).\ {}^{\sigma}C_{n+1}$.
Base case: n=1
$lhs = \sigma\{{}^{\sigma}C_1 - {}^{\sigma}C_0\} = \sigma(\sigma - 1)$
$rhs = 2.{}^{\sigma}C_2$. Therefore, $lhs = rhs$.
Induction step:
Assuming that it is true for $n = m$, we prove it for $n = m+1$.
$\sigma \sum_{i=m+1}^{0} (-1)^{m+1-i}.\ {}^{\sigma}C_i = -(m+1).\ {}^{\sigma}C_{m+1} + \sigma.\ {}^{\sigma}C_{m+1} = -\sigma.\ {}^{\sigma-1}C_m + \sigma.\ {}^{\sigma}C_{m+1} = \sigma.\ {}^{\sigma-1}C_{m+1} = (m+2).\ {}^{\sigma}C_{m+2}$

Based on this we have,
$\{(k-1).{}^{\sigma}C_{k-1} \sum_{i_1} z_{i_1} + (k-2).{}^{\sigma}C_{k-2} \sum_{i_1 \neq i_2} z_{i_1} z_{i_2} + ... + 1.{}^{\sigma}C_1 \sum_{i_1 \neq i_2 \neq ... \neq i_{k-1}} z_{i_1} z_{i_2} ... z_{i_{k-1}}\} =$
$\sigma \sum_{j=1}^{k-1} (-1)^{k-1-j} (b_{n-j} - {}^{\sigma}C_j)$
and the second equation of the theorem follows.

For n=even, we have $|a_{n/2}| = a_{n/2}/\sqrt{a_0}$. Note that this makes $|a_{n/2}| \in [-{}^{n}C_{n/2}, {}^{n}C_{n/2}]$ depending upon the choice of $\sqrt{a_0}$.
We therefore have,
$d|a_{n/2}|/dt = (1/\sqrt{a_0}) da_{n/2}/dt - (a_{n/2}/2a_0\sqrt{a_0}) da_0/dt$.
Inserting the values for $(da_{n/2}/dt)$ and (da_0/dt), we get
$d|a_{n/2}|/dt = (2\pi i/\Upsilon\sqrt{a_0})[\frac{n}{2}(a_{\frac{n}{2}} - (-1)^{\frac{n}{2}}.{}^{\sigma}C_{\frac{n}{2}}) + \sigma \sum_{j=1}^{\frac{n}{2}-1} (a_{n-j} - (-1)^j.{}^{\sigma}C_j) - a_{\frac{n}{2}} \frac{n-\sigma}{2}]$
The third equation results from simplifying this equation. It is easily verified that $d|a_{n/2}|/dt$ is equivalent to its conjugate, thus confirming that it is real.

The proof of the first equation is trivial.

QED.

Existence and Uniqueness proofs for the O.D.E with discontinuous r.h.s. defined in section 3.1

In section 3.1 we presented a discontinuous vector field $\mathcal{V}(p)$ on the phase space. We propose to demonstrate here that the solution to the *autonomous* differential equation with discontinuous r.h.s, $dp/dt = \mathcal{V}(p)$, can be defined in such a manner as to reflect the natural dynamics of the physical system described informally in the beginning of section 3.1.

As defined earlier, $p \in \langle {}^{1}\overline{\mathbb{L}}_{n_1} \times {}^{2}\overline{\mathbb{L}}_{n_2} \times ... \times {}^{\mathcal{S}}\overline{\mathbb{L}}_{n_{\mathcal{S}}} \rangle$. For the sake of brevity we denote the entire phase space by M and denote its tangent bundle by $T(M)$.

Definition 1 ***A domain of extensional support*** *for any point $p \in M$ is a set $\mathbb{E}$ that satisfies*
(i) $p \in \mathbb{E}$
(ii) $\mathbb{E}$ *with the subspace topology of M is C^k $(k \geq 1)$ diffeomorphic to a* bounded connected

open set U[31] *in* $\mathbb{R}^m$ *for* maximal[32] m.
(iii) The velocity field $\mathcal{V}$ *is* continuous *on* $\mathbb{E}$. *and,*
(iv) $\mathcal{V}(p) \in T_p(\mathbb{E})\ \forall p \in \mathbb{E}$.

We define a *local* solution to $\dot{p}(t) = \mathcal{V}(p)$ with initial condition $\langle p_0, t_0 \rangle$ as $\Psi(t)$ if
(i) $\Psi(t_0) = p_0$,
(ii) there exists a domain of extensional support $\mathbb{E}$ for $p_0 \in M$ and an interval I satisfying $t_0 \in I$ and $\{t \in I \Rightarrow \Psi(t) \in \mathbb{E}\}$, and
(iii) $\Psi(t)$ is *absolutely continuously differentiable* over I satisfying $\dot{\Psi}(t) = \mathcal{V}(\Psi(t))$ for all $t \in I$.

Since $\mathcal{V}$ is continuous and bounded on $\mathbb{E}$ there is a *continuation* of $\Psi(t)$ to a maximal interval of existence, and moreover, if (t_1, t_2) is such an interval then $\Psi(t)$ tends to the boundary of $\mathbb{E}$ as $t \to t_1$ or $t \to t_2$. Based on this we define additionally that
(iv) $\Psi(t_2) = \lim_{t \to t_2} \Psi(t)$, i.e., the point on $\partial\mathbb{E}$ that $\Psi(t)$ tends to as $t \to t_2$.

We are interested solely in the positive time solution to the differential equation and it is clear that by iterating on (ii), (iii), and (iv) above a piecewise absolutely continuously differentiable *global* solution can be constructed for positive time over all of M. Moreover, when $\mathcal{V}$ is bounded and continuous over all of M, the method reduces to the standard solution of the differential equation.

Definition 2 $\widetilde{\mathbb{E}}$ *is an* **extension** *of the domain of extensional support* $\mathbb{E}$ *for* p *if*
(i) $\widetilde{\mathbb{E}}$ *is a domain of extensional support for* p, *and*
(ii) $\widetilde{\mathbb{E}} \cap \mathbb{E}$ *is a domain of extensional support for* p.

Based on Peano's theorem we note that existence of a positive time solution for any initial condition $\langle p_0, t_0 \rangle \in M \times \mathbb{R}$ amounts to demonstrating that $\forall p \in M$, $\exists$ a domain of extensional support $\mathbb{E}$ for p. Moreover, if it can be demonstrated that $\mathbb{E}$ is *unique* till an extension and that $\mathcal{V}$ is *locally lipschitzian* on $\mathbb{E}$, then uniqueness of the solution follows from Picard-Lindelöf theorem.

The rest of the section is devoted to proving the above. We will show that $\mathcal{V}$ is continuously differentiable on $\mathbb{E}$ thereby making it locally lipschitzian. The proof is partitioned into two cases (a) $p \in M$ and $\forall i$, $p \notin P_i^I$ and (b) $p \in M$ and $\exists i$ such that $p \in P_i^I$.

(a) $p \in M$ and $\forall i$, $p \notin P_i^I$.

p is considered in terms of its projection $p = \langle p_1, p_2, ..., p_{\mathcal{S}} \rangle$, $p_i \in {}^i\overline{\mathbb{L}}_{n_i}$. For each i we choose $r_i = max\{x | p_i \in {}^i\overline{\mathbb{L}}^x_{n_i}, p_i \notin {}^i\overline{\mathbb{L}}^{x+1}_{n_i}\}$. We choose a bounded open set V in M such that (a) $p \in V$, (b) $\forall i$, $V \cap P_i^I = 0$, and (c) $\forall q_i \geq 0$, $V \cap \prod_{i=1}^{\mathcal{S}} {}^i\overline{\mathbb{L}}^{r_i+q_i}_{n_i} = 0$ whenever $\exists q_i \geq 1$. We set $\mathbb{E} = V \cap \prod_{i=1}^{\mathcal{S}} {}^i\overline{\mathbb{L}}^{r_i}_{n_i}$. If $\mathbb{E}$ is disconnected we choose the connected subset that contains p.

We prove that $\mathbb{E}$ is a domain of extensional support and unique till an extension.

[31] For any co-ordinate neighborhood $\langle V, \psi \rangle$ such that $p \in V$, $\psi(V \cap \mathbb{E})$ is C^k diffeomorphic to U.

[32] There is no $\mathbb{E}'$ such that $\mathbb{E}' \supset$ (*open set in* $\mathbb{E}$) and $dim(\mathbb{E}') > dim(\mathbb{E})$ such that $\mathbb{E}'$ satisfies (i), (ii), (iii), and (iv).

1. $\underline{p \in \mathbb{E}}$: $p \in V$, and $p \in \prod_{i=1}^{\mathcal{S}} {}^i\overline{\mathbb{L}}_{n_i}^{r_i}$.

2. $\underline{\mathbb{E} \text{ is } C^\infty \text{ diffeomorphic to a bounded open set in } \mathbb{R}^{\sum n_i - r_i}}$: We have already shown that $\prod_{i=1}^{\mathcal{S}} {}^i\overline{\mathbb{L}}_{n_i}^{r_i}$ is an imbedding in $\prod_{i=1}^{\mathcal{S}} {}^i\overline{\mathbb{L}}_{n_i}^{0}$. An appropriate $\langle V, \phi \rangle$ can therefore be chosen such that the diffeomorphism from $\mathbb{E}$ to U is a $\sum_{i=1}^{\mathcal{S}} n_i - r_i$ dimensional slice of an open set in $\mathbb{R}^{\sum n_i}$. Since V is bounded, we have U a bounded open set in $\mathbb{R}^{\sum n_i - r_i}$.

3. $\underline{\mathcal{V}(\mathbb{E}) \in T(\mathbb{E})}$: The informal description of the natural dynamics of the system (the flow) can be defined formally as a *local one-parameter group action* on $\mathbb{E}$. For each $p \in \mathbb{E}$ we choose an $I(p)$ such that $\forall t \in I(p)$, $\Psi(p,t) \in \mathbb{E}$. That such a non-empty interval exists for each p follows immediately from the informal description of the flow and the definition of $\mathbb{E}$ above. W is set to $\bigcup_{p \in \mathbb{E}} \{p\} \times I(p)$ making $\Psi : W \to \mathbb{E}$ the local one-parameter group action. When so defined, it becomes evident that $\mathcal{V}$ is the *infinitesimal generator* of Ψ. Therefore, $\mathcal{V}(\mathbb{E}) \in T(\mathbb{E})$.

4. $\underline{\mathcal{V} \text{ is continuous on } \mathbb{E}}$: It is obvious from the informal description of the flow that the local one-parameter group action Ψ just defined is C^∞ on W. $\mathcal{V}$ is therefore not only continuous but also C^∞ on $\mathbb{E}$.

5. $\underline{\mathbb{E} \text{ is of maximal dimension}}$: For $p \in M$ and a mapping $F : M \to M'$ to any arbitrary manifold M' we define continuity of F in direction $X_p \in T_p(M)$ at p as follows. We choose an arbitrary C^k ($k \geq 1$) function $f : I \subset \mathbb{R} \to M$ such that $f(0) = p$ and $\dot{f}(t)|_{t=0} = X_p$. If $F \circ f : I \to M'$ is continuous at $t = 0$ then F is continuous in direction X_p at p. It can be verified that the answers provided by all functions f that satisfy the above criteria are identical.

We now consider an $\mathbb{E}'$ of dimension greater than $\mathbb{E}$ such that $p = \langle p_1, p_2, ..., p_{\mathcal{S}} \rangle \in \mathbb{E}'$ and $\{open\ set\ in\ \mathbb{E}\} \subset \mathbb{E}'$. Consequently, $T(\mathbb{E}) \subset T(\mathbb{E}')$. Moreover, since $dim(\mathbb{E}) < dim(\mathbb{E}')$, $\exists X_p \in T_p(\mathbb{E}')$ such that $X_p \notin T_p(\mathbb{E})$. In other words, $X_p \in [\prod_{i=1}^{\mathcal{S}} T_{p_i}({}^i\overline{\mathbb{L}}_{n_i}^{0}) - \prod_{i=1}^{\mathcal{S}} T_{p_i}({}^i\overline{\mathbb{L}}_{n_i}^{r_i})]$. For any $f : I \to M$ that satisfies $f(0) = p$ and $\dot{f}(t)|_{t=0} = X_p$, $f(0+)$ and $f(0-)$ have at least one extra live spike for some neuron than $f(0)$. It follows from the natural dynamics of the system that $\mathcal{V}$ is discontinuous in the direction of X_p at p.

6. $\underline{\mathbb{E} \text{ is unique till an extension}}$: From the previous paragraph, any domain of extensional support $\mathbb{E}'$ can not have $X_p \in T(\mathbb{E}')$ such that $X_p \in [\prod_{i=1}^{\mathcal{S}} T_{p_i}({}^i\overline{\mathbb{L}}_{n_i}^{0}) - \prod_{i=1}^{\mathcal{S}} T_{p_i}({}^i\overline{\mathbb{L}}_{n_i}^{r_i})]$. The dimension of $\mathbb{E}'$ is therefore at most $\sum_{i=1}^{\mathcal{S}} n_i - r_i$. Moreover, for any $p' \in M$ such that $p' \notin \prod_{i=1}^{\mathcal{S}} {}^i\overline{\mathbb{L}}_{n_i}^{r_i} - {}^i\overline{\mathbb{L}}_{n_i}^{r_i+1}$ or $p' \in P_i^I$, we have $p' \notin \mathbb{E}'$ because $\mathcal{V}$ is discontinuous on any path from p to p'. It therefore follows from the above discussion that $\mathbb{E}'$ is a connected open set in $\prod_{i=1}^{\mathcal{S}} {}^i\overline{\mathbb{L}}_{n_i}^{r_i} - {}^i\overline{\mathbb{L}}_{n_i}^{r_i+1}$ containing p such that $\forall i\ \mathbb{E}' \cap P_i^I = 0$. $\mathbb{E}' \cap \mathbb{E}$ is therefore also a domain of extensional support for p.

7. $\underline{\mathcal{V} \text{ is locally lipschitzian on } \mathbb{E}}$: Follows trivially from the fact that $\mathcal{V}$ is C^∞ on $\mathbb{E}$.

(b) $p \in M$ and $\exists i, p \in P_i^I$.

As in the previous case, p is considered in terms of its projection $p = \langle p_1, p_2, ..., p_{\mathcal{S}} \rangle$, $p_i \in {}^i\overline{\mathbb{L}}_{n_i}$. Once again, for each i we choose $r_i = max\{x | p_i \in {}^i\overline{\mathbb{L}}^x_{n_i}, p_i \notin {}^i\overline{\mathbb{L}}^{x+1}_{n_i}\}$. Without loss of generality we assume that $p \in P^I_i$ for $i = 1...k$ and $p \notin P^I_i$ for $i = (k+1)...\mathcal{S}$.

For each $j = 1...k$ we construct the hyper-surface $(\prod_{i=1}^{k} {}^i\overline{\mathbb{L}}^{r_i - q^j_i}_{n_i} \times \prod_{i=k+1}^{\mathcal{S}} {}^i\overline{\mathbb{L}}^{r_i}_{n_i}) \cap P^I_j$ where $q^j_i = 1$ for $i = 1...k$, $i \neq j$ and $q^j_i = 0$ for $i = j$. Recall that $\forall i$, ${}^i\overline{\mathbb{L}}^{r_i}_{n_i} \subset {}^i\overline{\mathbb{L}}^{r_i - 1}_{n_i}$. By construction each hyper-surface is C^1. For each $j = 1...k$ we choose a bounded open set (induced topology) $\widetilde{\mathbb{Z}}_j$ on the corresponding hyper-surface such that (a) $p \in \widetilde{\mathbb{Z}}_j$, (b) $\widetilde{\mathbb{Z}}_j \cap P^I_i = 0$ for $i = (k+1)...\mathcal{S}$, and (c) $\forall q_i \geq 0$, $\widetilde{\mathbb{Z}}_j \cap \prod_{i=1}^{\mathcal{S}} {}^i\overline{\mathbb{L}}^{r_i + q_i}_{n_i} = 0$ whenever $\exists q_i \geq 1$.

On each $\widetilde{\mathbb{Z}}_j$ $(j = 1...k)$ we define the following functions. It can easily be verified that each of these functions are continuous.

(i) ${}^j h^A_i(p')$ (defined only for $i = 1...k, i \neq j$): The domain of the function is restricted to $p' \in \widetilde{\mathbb{Z}}_j$. ${}^j h^A_i(p') = {}^j h^A_i(p'_i)$ is defined as $\Upsilon_i.\Delta$ wherein Δ is the *smallest positive* real such that when p'_i is represented as roots on the unit circle S^1, and exactly $(r_i - 1)$ roots lying on e^{i0} are disregarded[33], at least one of the remaining roots lies in the interval $[e^{i\Delta}, e^{-i\Delta}]$. In other words, it is the absolute value of the argument of the root lying closest to e^{i0} when exactly $(r_i - 1)$ roots lying on e^{i0} are disregarded. Naturally the value of the function is zero for all p'_i that correspond to more than $(r_i - 1)$ roots lying on e^{i0}, like for example at p.

(ii) ${}^j h^B_i(p')$: (defined only for $i = j, (k+1), ...\mathcal{S}$): The domain of the function is once again restricted to $p' \in \widetilde{\mathbb{Z}}_j$. ${}^j h^B_i(p') = {}^j h^B_i(p'_i)$ is defined in similar terms as $\Upsilon_i.\Delta$ wherein Δ is the *smallest positive* real such that when p'_i is represented as roots on the unit circle S^1, and exactly r_i roots lying on e^{i0} are disregarded, at least one of the remaining roots lies in the interval $[e^{i\Delta}, e^{-i\Delta}]$.

(iii) ${}^j h^A(p')$: The domain is restricted to $p' \in \widetilde{\mathbb{Z}}_j$. ${}^j h^A(p') = max_{i=1...k, i \neq j}\{{}^j h^A_i(p')\}$.

(iv) ${}^j h^B(p')$: The domain is restricted to $p' \in \widetilde{\mathbb{Z}}_j$. ${}^j h^B(p') = min_{i=j,(k+1),...\mathcal{S}}\{{}^j h^B_i(p')\}$.

We now define the following limits. These limits exist because the functions in question are bounded and continuous, and the respective domains are bounded.
(iv) ${}^j\Gamma^A(\widetilde{\mathbb{Z}}_j) = l.u.b\{{}^j h^A(p') | p' \in \widetilde{\mathbb{Z}}_j\}$.
(v) ${}^j\Gamma^B(\widetilde{\mathbb{Z}}_j) = g.l.b\{{}^j h^B(p') | p' \in \widetilde{\mathbb{Z}}_j\}$.
It follows immediately that $lim_{radius(\widetilde{\mathbb{Z}}_j) \to 0} {}^j\Gamma^A(\widetilde{\mathbb{Z}}_j) = 0$ and $lim_{radius(\widetilde{\mathbb{Z}}_j) \to 0} {}^j\Gamma^B(\widetilde{\mathbb{Z}}_j) > 0$.

For each $j = 1...k$, we choose an open set $\mathbb{Z}_j \subset \widetilde{\mathbb{Z}}_j$ that satisfies, (a) $p \in \mathbb{Z}_j$, and (b) ${}^j\Gamma^B(\mathbb{Z}_j) > {}^j\Gamma^A(\mathbb{Z}_j)$. In addition, we set $I_j = (-{}^j\Gamma^A(\mathbb{Z}_j) : {}^j\Gamma^A(\mathbb{Z}_j))$.

We now define $\theta_j : \mathbb{Z}_j \times I_j \to \prod_{i=1}^{k} {}^i\overline{\mathbb{L}}^{r_i - 1}_{n_i} \times \prod_{i=k+1}^{\mathcal{S}} {}^i\overline{\mathbb{L}}^{r_i}_{n_i}$, a function that for any $t \in I_j$ takes $p' = \langle p'_1, p'_2, ..., p'_{\mathcal{S}} \rangle \in \mathbb{Z}_j$ to $p'' = \langle p''_1, p''_2, ..., p''_{\mathcal{S}} \rangle \in \prod_{i=1}^{k} {}^i\overline{\mathbb{L}}^{r_i - 1}_{n_i} \times \prod_{i=k+1}^{\mathcal{S}} {}^i\overline{\mathbb{L}}^{r_i}_{n_i}$ wherein each p''_i for $i = 1...k$ when represented as roots on the unit circle is the result of multiplying by $e^{i\frac{t}{\Upsilon_i}}$ all roots corresponding to p'_i (when represented as roots on the unit circle) *except*

[33] There are at least $(r_i - 1)$ roots on e^{i0} $\forall p' \in \widetilde{\mathbb{Z}}_j$.

exactly $(r_i - 1)$ roots lying at e^{i0}, and each p_i'' for $i = (k+1)...\mathcal{S}$ when represented as roots on the unit circle is the result of multiplying by $e^{i\frac{t}{\Upsilon_i}}$ all roots corresponding to p_i' *except* exactly r_i roots lying at e^{i0}. We denote the image set $\{p''|p'' = \theta_j(p', t), p' \in \mathbb{Z}_j, t \in I_j\}$ by $\mathbb{Z}_j(I_j)$. If $\mathbb{Z}_j(I_j) \cap P_i^I \neq 0$ for some $i = (k+1)...\mathcal{S}$, we adjust the interval I_j to make it so. Finally, we set $\mathbb{E} = \bigcap_{j=1...k} \mathbb{Z}_j(I_j)$.

We prove that $\mathbb{E}$ is a domain of extensional support and unique till an extension.
1. $p \in \mathbb{E}$: $p \in \mathbb{Z}_j$, and $0 \in I_j$ for $j = 1...k$. Therefore $p \in \mathbb{Z}_j(I_j)$ for $j = 1...k$.

2. $\mathbb{E}$ is C^k $(k \geq 1)$ diffeomorphic to a bounded open set in $\mathbb{R}^m$: $\forall i, P_i^I$ is a C^1 hyper-surface. Therefore, so are $\mathbb{Z}_j$ and $\mathbb{Z}_j(I_j)$ for $j = 1...k$. $\mathbb{E}$ is bounded trivially because of the compactness of M.

3. $\mathcal{V}(\mathbb{E}) \in T(\mathbb{E})$: We make the following observations: (a) On any $\mathbb{Z}_j(I_j)$ for $j = 1...k$ the only points $p = \langle p_1, p_2, ..., p_{\mathcal{S}} \rangle$ where $p_j \in {}^j\overline{\mathbb{L}}_{n_j}^{r_j}$ is at $t = 0$ or on $\mathbb{Z}_j$. (b) For any $j = 1...k$ the only points p for which $\theta_j(.)$ defined above might not match the natural flow of the system $\Psi(.)$ is when $p_i \in {}^i\overline{\mathbb{L}}_{n_i}^{r_i}$ for $i = 1...k$. However, by construction $p \in \mathbb{E} \Rightarrow p \in \mathbb{Z}_j(I_j)$ for $j = 1...k$ and based on (a) therefore, such a p satisfies $p_i \in \mathbb{Z}_i \subset P_i^I$. It follows that $\theta_j(.)$ does match $\Psi(.)$ for all $p \in \mathbb{E}$. (c) Any $p^a \in \mathbb{Z}_a$ and $p^b \in \mathbb{Z}_b$ $(a \neq b)$ that satisfy $\theta_a(p^a, t_1) = \theta_b(p^b, t_2)$ also satisfy $\theta_a(p^a, t_1 + \Delta t) = \theta_b(p^b, t_2 + \Delta t)$ when $t_1, t_1 + \Delta t \in I_a$ and $t_2, t_2 + \Delta t \in I_b$. Informally, this means that the θ_j's are consistent. (d) Since each I_j is an open set, for each $p \in \mathbb{E}$, $\exists I$ an interval such that $\theta_j(p, t) \in \mathbb{Z}_j(I_j)$ for $t \in I$ for all $j = 1...k$.

Based on these observations we note that $\mathcal{V}$ is the infinitesimal generator for the local one-parameter group action defined by θ.

4. $\mathcal{V}$ is continuous on $\mathbb{E}$: It is obvious from the construction of the local one-parameter group actions $\theta_j(.)$ for $j = 1...k$ that they are at least C^1 on $\mathbb{E}$.

5 and 6. $\mathbb{E}$ is of maximal dimension and is unique till an extension: We make the following observations. (a) For any point p' such that $p' \in M$ and $p' \notin \prod_{i=1}^{k} {}^i\overline{\mathbb{L}}_{n_i}^{r_i - 1} \times \prod_{i=k+1}^{\mathcal{S}} {}^i\overline{\mathbb{L}}_{n_i}^{r_i}$, $\mathcal{V}$ is discontinuous on any path from p to p' implying that any domain of extensional support $\mathbb{E}' \subset \prod_{i=1}^{k} {}^i\overline{\mathbb{L}}_{n_i}^{r_i - 1} \times \prod_{i=k+1}^{\mathcal{S}} {}^i\overline{\mathbb{L}}_{n_i}^{r_i}$. (b) $(\mathbb{E} \cap \prod_{i=1}^{\mathcal{S}} {}^i\overline{\mathbb{L}}_{n_i}^{r_i})$ is an open set in $(\prod_{i=1}^{\mathcal{S}} {}^i\overline{\mathbb{L}}_{n_i}^{r_i} \bigcap_{i=1}^{k} P_i^I)$. (c) For any point p' such that $p' \in \prod_{i=1}^{\mathcal{S}} {}^i\overline{\mathbb{L}}_{n_i}^{r_i}$ and $p' \notin P_i^I$ for some $i = 1...k$, $\mathcal{V}$ is discontinuous on any path from p to p'. Therefore, when attention is restricted to the submanifold $\prod_{i=1}^{\mathcal{S}} {}^i\overline{\mathbb{L}}_{n_i}^{r_i}$, $\mathbb{E} \cap \prod_{i=1}^{\mathcal{S}} {}^i\overline{\mathbb{L}}_{n_i}^{r_i}$ is not only of maximal dimension but also unique till an extension (it being an open set in the referred space).

We now prove by induction that $\mathbb{E}$ is of maximal dimension and unique till an extension.
Base case: k=1
Let $p \in P_i^I$ for i=1. From (a) above any $\mathbb{E}' \subset {}^1\overline{\mathbb{L}}_{n_1}^{r_1 - 1} \times \prod_{i=2}^{\mathcal{S}} {}^i\overline{\mathbb{L}}_{n_i}^{r_i}$. Also from (c) above $\mathbb{E} \cap \prod_{i=1}^{\mathcal{S}} {}^i\overline{\mathbb{L}}_{n_i}^{r_i} \equiv \mathbb{Z}_1$ is not only of maximal dimension in the referred space but also unique till an extension. $\mathbb{Z}_1$ in itself is not a domain of extensional support because $\mathcal{V} \notin T(\mathbb{Z}_1)$. $\mathbb{Z}_1(I_1) \supset \mathbb{Z}_1$ however is, and furthermore, is of dimension one greater than $\mathbb{Z}_1$ and lies in ${}^1\overline{\mathbb{L}}_{n_1}^{r_1 - 1} \times \prod_{i=2}^{\mathcal{S}} {}^i\overline{\mathbb{L}}_{n_i}^{r_i}$. This proves that $\mathbb{E}$ is of maximal dimension.

Let $\mathbb{E}'$ be a domain of extensional support that contains a point p' not in any extension of $\mathbb{E}$. Since $\mathcal{V}$ on $[{}^1\overline{\mathbb{L}}_{n_1}^{r_1-1} - {}^1\overline{\mathbb{L}}_{n_1}^{r_1}] \times \prod_{i=2}^{\mathcal{S}} {}^i\overline{\mathbb{L}}_{n_i}^{r_i}$ in the vicinity of p is differentiable, based on (c), $\mathbb{E}'$ must contain a trajectory passing through p' that intersects $\prod_{i=1}^{\mathcal{S}} {}^i\overline{\mathbb{L}}_{n_i}^{r_i}$ outside $\prod_{i=1}^{\mathcal{S}} {}^i\overline{\mathbb{L}}_{n_i}^{r_i} \cap P_i^I$ contradicting the assumption that $\mathbb{E}'$ is a domain of extensional support.

Induction step:

Assuming that it is true for $k-1$ we prove it for k.

In other words, we assume that the situation is altered by the materialization of P_k^I in such a manner that now $p \in P_k^I$ additionally. We denote the respective domains of extensional support by $\mathbb{E}_{k-1}$ and $\mathbb{E}_k$. To begin with, we note that $\mathbb{E}_{k-1} \subset \prod_{i=1}^{k-1} {}^i\overline{\mathbb{L}}_{n_i}^{r_i-1} \times \prod_{i=k}^{\mathcal{S}} {}^i\overline{\mathbb{L}}_{n_i}^{r_i}$ and $\mathbb{E}_k \subset \prod_{i=1}^{k} {}^i\overline{\mathbb{L}}_{n_i}^{r_i-1} \times \prod_{i=k+1}^{\mathcal{S}} {}^i\overline{\mathbb{L}}_{n_i}^{r_i}$.

We claim that for the case of $p \in P_i^I$ for $i = 1...k$, when attention is restricted to the subspace $\prod_{i=1}^{k-1} {}^i\overline{\mathbb{L}}_{n_i}^{r_i-1} \times \prod_{i=k}^{\mathcal{S}} {}^i\overline{\mathbb{L}}_{n_i}^{r_i}$, $\mathbb{E}_{k-1} \cap P_k^I$ is not only of maximal dimensionality but also unique till an extension. This follows from the following observations.

(a) When $p \in P_i^I$ for $i = 1...k$, and attention is restricted to $\prod_{i=1}^{k-1} {}^i\overline{\mathbb{L}}_{n_i}^{r_i-1} \times \prod_{i=k}^{\mathcal{S}} {}^i\overline{\mathbb{L}}_{n_i}^{r_i}$, points in the domain of extensional support must lie on P_k^I.

(b) Suppose $\mathbb{E}_{k-1} \cap P_k^I$ is not maximal and instead $\mathbb{E}'_{k-1} \cap P_k^I$ is. Both $\mathbb{E}_{k-1}$ and $\mathbb{E}'_{k-1}$ are subsets of $\prod_{i=1}^{k-1} {}^i\overline{\mathbb{L}}_{n_i}^{r_i-1} \times \prod_{i=k}^{\mathcal{S}} {}^i\overline{\mathbb{L}}_{n_i}^{r_i}$, and it is clear that if we revert to the case wherein $p \in P_i^I$ for $i = 1...(k-1)$, both $\mathbb{E}_{k-1}$ and $\mathbb{E}'_{k-1}$ satisfy all requirements for being a domain of extensional support, and furthermore, $\mathbb{E}'_{k-1}$ is not an extension of $\mathbb{E}_{k-1}$ contradicting the assumption that $\mathbb{E}_{k-1}$ is unique till an extension.

(c) It follows that if $\mathbb{E}'_{k-1}$ does exist, it must be an extension of $\mathbb{E}_{k-1}$, which in turn makes $\mathbb{E}_{k-1} \cap P_k^I$ unique till an extension.

The rest of the argument is identical to that of the base case. We extend $\mathbb{E}_{k-1} \cap P_k^I$ into $\prod_{i=1}^{k} {}^i\overline{\mathbb{L}}_{n_i}^{r_i-1} \times \prod_{i=k+1}^{\mathcal{S}} {}^i\overline{\mathbb{L}}_{n_i}^{r_i}$ to produce $[\mathbb{E}_{k-1} \cap P_k^I](I_k)$. The argument for demonstrating that this is a domain of extensional support unique till an extension for the case of $p \in P_i^I$ for $i = 1...k$ is identical to that of the base case. Finally, we note that by construction $[\mathbb{E}_{k-1} \cap P_k^I](I_k)$ is an extension of $\mathbb{E}_k$.

7. $\mathcal{V}$ is locally lipschitzian on $\mathbb{E}$: It is obvious that $\mathcal{V}$ is differentiable on $\mathbb{E}$.

References

[1] Abeles, M. (1982) Local Cortical Circuits- An Electrophysiological Study. Braitenberg V. (Ed.) Studies of Brain Function. Springer, Berlin Heidelberg New York.

[2] Aertsen, A. and Braitenberg, V. (Eds.) (1992) Information Processing in the Cortex: Experiments and Theory. Springer-Verlag, Berlin Heidelberg New York.

[3] Babloyantz, A., Nicolis, C., and Salazar, M. (1985) Evidence of Chaotic Dynamics of Brain Activity During the Sleep Cycle. Phys. Lett.(A), 111, pp. 152-156.

[4] Babloyantz, A. (1990) Chaotic Dynamics in Brain Activity. Basar E. (Ed.) Chaos in Brain Function. Springer-Verlag, Berlin Heidelberg New York, pp. 42-48.

[5] Bair, W. and Koch, C. (1996) Temporal Precision of Spike Trains in Extrastriate Cortex of the Behaving Monkey. Neural Computation, 8, pp. 1185-1198.

[6] Basar, E. (Ed.) (1990) Chaos in Brain Function. Springer-Verlag, Berlin Heidelberg New York.

[7] Bernander, O., Douglas, R. J., and Koch, C. (1992) A Model of Regular-Firing Cortical Pyramidal Neurons. CNS Memo 16, California Institute of Technology, Computational and Neural Systems Program.

[8] Braitenberg, V. (1978) Cortical Architectonics: General and Area. Brazier M. A. B. and Petsche H. (Eds.) Architectonics of the Cerebral Cortex. Raven, New York, pp. 443-465.

[9] Braitenberg, V. and Schüz, A. (1991) Anatomy of the Cortex: Statistics and Geometry. Springer-Verlag, Berlin Heidelberg New York.

[10] Cohn, A. (1922) Uber die Anzahl der Wurzeln einer algebraischen Gleichung in einem Kreise. Math Zeit, 14, pp. 110-148.

[11] Coolidge, J. L. (1908) The continuity of the roots of an algebraic equation. Annals of Math, (series 2), 9, pp. 116-118.

[12] Erb, M., and Aertsen, A. (1992) Dynamics of Activity in Biology- Oriented Neural Network Models: Stability at Low Firing Rates. Aertsen and Braitenberg (Eds.) Information Processing in the Cortex. Springer-Verlag, Berlin Heidelberg New York, pp. 201-223.

[13] Evarts, E. V. (1964) Temporal Patterns of Discharge of Pyramidal Tract Neurons During Sleep and Waking in the Monkey. Jour. Neurophysiol., 27, pp. 152-171.

[14] Fatt, P. and Katz, B. (1952) Spontaneous Subthreshold Activity at Motor Nerve Endings. Jour. Physiol., 117, pp. 109-128.

[15] Fitzhugh, R. (1961) Impulses and Physiological States in Theoretical Models of Nerve Membrane. Biophys. Jour., 1, pp. 445-466.

[16] Fodor, J. A. and Pylyshyn, Z. W. (1988) Connectionism and Cognitive Architecture: A Critical Analysis. Cognition, 28, pp. 3-71.

[17] Grevins, A. S. and Shaffer, R. E. (1980) A Critical Review of Electroencephalographic (EEG) Correlates of Higher Cortical Functions. CRC Critical Rev. Bioeng., 4(2), pp. 113-163.

[18] Hebb, D. O. (1949) Organization of Behavior. A Neurophysiological Theory. Wiley & Sons, New York.

[19] Hines, M. (1993) NEURON - A Program for Simulation of Nerve Equations. Neural Systems: Analysis and Modeling, F. Eckman(ed.), Kluwer, pp. 127-136.

[20] Hodgkin, A. L. and Huxley, A. F. (1952a) Currents Carried by Sodium and Pottasium Ions through the Membrane of a Giant Axon of Loligo. Jour. Physiol., 116, pp. 449-472.

[21] Hodgkin, A. L. and Huxley, A. F. (1952b) The Components of Membrane Conductance in the Giant Axon of Loligo. Jour. Physiol., 116, pp. 473-496.

[22] Hodgkin, A. L. and Huxley, A. F. (1952c) The Dual Effect of Membrane Potential on Sodium Conductance in the Giant Axon of Loligo. Jour. Physiol., 116, pp. 497-506.

[23] Hodgkin, A. L. and Huxley, A. F. (1952d) A Quantitative Description of Membrane Current and its Application to Conduction and Excitation in Nerve. Jour. Physiol., 117, pp. 500-544.

[24] Hubel, D. H. and Wiesel, T. N. (1965) Receptive Fields and Functional Architecture in Two Non-striate Visual Areas (18 and 19) of the Cat. Jour. Neurophysiol., 28, pp. 229-289.

[25] Jasper, H. H. (1981) Problems of Relating Cellular or Modular Specificity to Cognitive Functions: Importance of State Dependent Reactions. Schmitt F. O., Worden F. G., Adelman G., and Dennis S. G. (Eds.) The Organization of the Cerebral Cortex. MIT Press, Cambridge, pp. 375-393.

[26] Krüger, J. (1983) Simultaneous Individual Recordings from Many Cerebral Neurons: Techniques and Results. Rev. Physiol. Biochem. Pharmacol., 98, pp. 177-229.

[27] Krüger, J. (Ed.) (1990a) Neuronal Cooperativity. Springer-Verlag, Berlin Heidelberg New York.

[28] Krüger, J. (1990b) Spike Train Correlation on Slow Time Scales in Monkey Visual Cortex. Krüger, J (Ed.) Neuronal Cooperativity. Springer-Verlag, Berlin Heidelberg New York.

[29] MacGregor, R. J. and Lewis, E. R. (1977) Neural Modeling, Plenum Press, New York.

[30] Mainen, Z. F. and Sejnowski, T. J. (1995) Reliability of Spike Timing in Neocortical Neurons. Science, 268, pp. 1503-1507.

[31] Marden, M. (1948) The Number of Zeros of a Polynomial in a Circle. Proc. Nat. Acad. Sci. U.S.A, 34, pp. 15-17.

[32] McCulloch, W. S. and Pitts, W. (1943) A Logical Calculus of the Ideas Immanent in Nervous Activity. Bull. Math. Biophys, 5, pp. 115-133.

[33] Minsky, M. and Papert, S. (1972) Perceptrons. MIT Press, Cambridge, Mass.

[34] Mountcastle, V. B. (1957) Modality and Topographic Properties of Single Neurons of Cat's Somatic Sensory Cortex. Jour. Neurophysiol., 20, pp. 408-434.

[35] Nagumo, J. S., Arimoto, S. and Yoshizawa, S. (1962) An Active Pulse Transmission Line Simulating Nerve Axon. Proc. I. R. E., 50, pp. 2061-2070.

[36] Newell, A. (1980) Physical Symbol Systems. Cognitive Science, 4, pp. 135-183.

[37] Newell, A. and Simon, H. A. (1976) Computer Science as Empirical Inquiry: Symbols and Search. Comm. of the ACM, 19, pp. 113-126.

[38] Peters, A. and Proskauer, C. C. (1980) Synaptic Relationships between a Multipolar Stellate Cell and a Pyramidal Neuron in the Rat Visual Cortex: A Combined Golgi-Electron Microscope Study. Jour. Neurocytol., 9, pp. 163-183.

[39] Rall, W. (1960) Membrane Potential Transients and Membrane Time Constants of Motoneurons, Exp. Neurol., 2, pp. 503-532.

[40] Ricciardi, L. M. (1977) Diffusion Processes and Related Topics in Biology. Springer, Berlin.

[41] Röschke, J. and Basar, E. (1989) Correlation Dimensions in Various Parts of Cat and Human Brain in Different States. Basar E. and Bullock T. H. (Eds.) Brain Dynamics, Springer, Berlin. pp. 131-148.

[42] Rosenblatt, F. (1958) The Perceptron, a Probabilistic Model for Information Organization and Storage in the Brain. Psych. Rev., 65, pp. 368-408.

[43] Rumelhart, D. E., Hinton G. E. and Williams R. J. (1986) Learning Internal Representations by Error Propagation. Parallel Distributed Processing, pp. 318-362.

[44] Rumelhart, D. E. and McClelland, J. L. (1986) PDP Models and General Issues in Cognitive Science. Parallel Distributed Processing(I and II), MIT Press, Cambridge, Mass.

[45] Sampath, G. and Srinivasan, S. K. (1977) Stochastic Models for Spike Trains of Single Neurons. Springer, Berlin.

[46] Softky, W. R. and Koch, C. (1992) Cortical Cells Should Fire Regularly, But Do Not. Neural Computation, 4, pp. 643-646.

[47] Schüz, A. (1992) Randomness and Constraints in the Cortical Neuropil. Aertsen and Braitenberg (Eds.) Information Processing in the Cortex. Springer-Verlag, Berlin Heidelberg New York, pp. 3-21.

[48] Tuckwell, H. C. (1988) Introduction to Theoretical Neurobiology, Volume I, Cambridge Univ Press, Cambridge New York.

[49] Walsh, J. B. and Tuckwell, H. C. (1985) Determination of the Electrical Potential over Dendritic Trees by Mapping onto a Nerve Cylinder, Jour. Theoret. Neurobiol., 4, pp. 27-46.